

Hydrodenitrogenation of Quinoline and Coal Using Transition Metal Sulfides

Christine W. Curtis and Donald R. Cahela

Chemical Engineering Department, Auburn
University, Alabama 36849

This study investigates the effectiveness of unsupported, precipitated transition metal sulfides as HYD and HDN catalysts in both a quinoline system and a coal liquefaction system. The transition metal sulfides of moderate surface areas were produced by a method developed by Chianelli and Dines (1) in the late 1970's. These materials crystallize in weakly interacting layers which allow for ready intercalation of appropriate species. A number of different transition metal sulfides have been tested for HDS activity using dibenzothiophene (2) and are good candidates for hydrodenitrogenation (HDN) studies. The degree of HYD and HDN of quinoline and the reaction products from coal liquefaction were determined using precipitated transition metal sulfides and compared to commercial transition metal sulfides, commercial hydrotreating catalysts such as CoMo/Al₂O₃ and NiMo/Al₂O₃, and platinum containing catalysts such as Pt/SiO₂ and PtS₂.

Experimental

Preparation of Catalysts. Each precipitated transition metal sulfide was prepared by dissolving the metal chloride in ethyl acetate (EA) which was then added to a slurry of lithium sulfide (Li₂S), precipitating the metal sulfide. The product was annealed with pure H₂S at 400°C, washed with 12% acetic acid and then sulfided with 10% H₂S/H₂ at 400°C for 1 hour. The metal chlorides used were CrCl₃, MoCl₄, WCl₆, FeCl₃ and RuCl₃·3H₂O, producing Cr₂S₃, MoS₂, WS₂, FeS_x and RuS₂. All of the chemicals required for synthesis were obtained from Alfa Chemicals.

The composition of the metal sulfides was confirmed by X-ray diffraction by matching the d spacings of the sample with the reference. The experimental data matched the standards sufficiently to confirm the identity of the metal sulfides listed above. Sulfur analyses of both the precipitated and commercial transition metal sulfides are compared to the theoretical in Table 1. Surface area measurements by dynamic B.E.T. using N₂ in He are also given in Table 1. Differences in the surface areas of different batches of a given transition metal sulfide reflect the sensitivity of the surface area to preparation methods.

A platinum on silica (Pt/SiO₂) catalyst was prepared by adding 0.44 g SiO₂ to 12.46 g of a 5% solution of hydroplatanic acid. Water was removed by vacuum rotary evaporation and the catalyst was dried for 16 hr at 50°C under 25 mm Hg. After grinding, the Pt/SiO₂ was reduced in a 40 ml/min H₂ flow producing a silvery black material. PtS₂ was obtained from Alfa Chemicals. The NiMo/Al₂O₃ and CoMo/Al₂O₃ catalysts were presulfided in a stream of 10 volume percent H₂S in H₂; sulfiding was begun at 250°C and the temperature was raised by 50°C every fifteen minutes until 400°C was reached and maintained for one hour. Both catalysts were ground before use.

Quinoline Model System. Reactions were performed with the precipitated and commercial transition metal sulfides, Pt/SiO₂, PtS₂, CoMo/Al₂O₃ and NiMo/Al₂O₃ catalysts in 15 cm³ stainless steel tubing bomb reactors. Two weight percent quinoline in hexadecane was used as the reactant solution (5 g) with 0.025 g catalyst and 1250 psi hydrogen (cold). The reactor was maintained at 380°C while being agitated at 850 rpm. Most of the reactions were at least duplicated. Several lower temperatures were used with the Pt/SiO₂ catalyst. The liquid products were analyzed by gas chromatography using a fused silica 30 m capillary DB-5 column with a 0.2 micron film with FID detection and p-xylene as the internal standard. NH₃ was analyzed using a Chromosorb 103 column and TCD detection. Hydrogen consumption was determined using a molecular sieve column with TCD detection in conjunction with standard PVT methods.

Table 1. Analysis of Catalysts

Catalyst	Sulfur, %		Surface Area, m ² /g
	Sample	Theoretical	
Cr ₂ S ₃ -4	44.0	48.1	19.5
Cr ₂ S ₃ -C	49.6	48.1	12.5
MoS ₂ -3	37.7	40.1	30.8
MoS ₂ -7		40.1	24.1*
MoS ₂ -C	41.1	40.1	10.7
WS ₂ -2	25.1	25.9	13.5
WS ₂ -4		25.9	
WS ₂ -C	24.9	25.9	8.5
FeS-2	39.1	36.5	6.7
FeS ₂ -C	57.2	53.5	4.9
RuS ₂ -3	30.2	38.8	26.4*
			19.4
RuS ₂ -5			81.5*
NiMo/Al ₂ O ₃			174
CoMo/Al ₂ O ₃			180

*Analyses performed by Quantachrome Corporation

The concentration of the liquid phase products is given for each compound as a mole percentage of quinoline initially charged to the reactor. The data is summarized in terms of percent of maximum hydrogenation (PMH), percent hydrodenitrogenation (PHDN), and percent hydrogenolysis (PHYG). PMH is the number of moles of hydrogen required to produce the observed product distribution from quinoline as a percentage of the hydrogen required to produce the final end product, propylcyclohexane (PCH). PHDN is calculated by summing the mole percentage for the components which do not contain nitrogen. PHYG is obtained by summing the mole percentages for the compounds which have resulted from hydrogenolysis of the C-N bond.

Coal Liquefaction Reactions. Ground Kentucky #11 coal with a nitrogen content of 1.10% was used in the liquefaction reactions. Two batches of coal were used: Batch A, kept in a desiccator, dried during the course of the experiments, while the moisture content of Batch B remained fairly constant. Thermal and several catalytic reactions were performed using Batch A; the product distributions were corrected for the changing moisture composition of the coal.

Coal liquefaction reactions were performed with MoS₂, RuS₂, NiMo/Al₂O₃, and Pt/SiO₂ as well as thermally in 46 cc stainless steel tubing bomb reactors. The charge to the reactor was 0.5 g of coal with 0.5 g anthracene as solvent. Reactions were performed at 425°C for 60 minutes at an agitation rate of 850 rpm. Recovery of the product from the reactor was based upon the weights of the solid and liquid fractions. In calculating the product distributions, all losses were equally distributed among the solid and liquid fractions. The product distribution is reported on a maf coal basis.

The liquid and solid products were separated by sequential washing with methylene chloride - methanol (9:1 v/v) solution (MCM) and tetrahydrofuran (THF). This separation produced three fractions: MCM solubles (MCMS), MCM insolubles-THF solubles (THFS) and THF insolubles or ash-free insoluble organic matter (IOM). The MCMS fraction was further fractionated by the chromatographic method of Boduszynski et al.(3) into compound-class fractions: hydrocarbons (HC), nitrogen heterocycles (NH), hydroxylaromatics (HA) and polyfunctional compounds (PC). Model compounds such as anthracene, acridine, carbazole and 2-naphthol, were chromatographed and verified the procedure. The hydrocarbon fraction separated from the MCMS fraction was further analyzed for anthracene hydrogenation products using the same capillary column as for quinoline. The sample, dissolved in toluene with phenanthrene as the internal standard, was analyzed isothermally at

180°C. Anthracene and three major hydrogenation products were observed: 9,10-dihydroanthracene (DHA), 1,4,5,8,9,10-hexahydroanthracene (HHA), and 1,2,3,4,5,6,7,8-octahydroanthracene. In some reactions, a corrected sum (CRS) is used which includes the light cracked products produced during the reaction assuming a response factor of unity and disregarding molecular weight changes. This CRS was required to obtain reasonable recovery values due to cracking of anthracene during the reaction. The anthracene products are reported as a percentage of the anthracene charged, the sum of which represents the recovered anthracene.

Results and Discussion

The activity and selectivity of precipitated transition metal sulfides for HDN of quinoline were compared to that of NiMo/Al₂O₃, CoMo/Al₂O₃, commercial transition metal sulfides and Pt/SiO₂. Several transition metals from groups 6B and 8A were chosen. The catalysts which showed the highest level of HYD and HDN activity in the quinoline system were used for the coal liquefaction reactions. Quinoline Reaction System. The reaction pathway (Figure 1) for quinoline under catalytic conditions has been extensively investigated by Satterfield and coworkers (4-6). In the current study, the gaseous and liquid products from both thermal and catalytic reactions were analyzed and reasonable recoveries of the liquid products were attained. Methane (CH₄) was the only hydrocarbon gas observed. The ammonia (NH₃) observed was usually much less than it should have been based upon the denitrogenation of the liquid products. Solubility experiments in hexadecane showed that ~70% of the hexadecane was absorbed by the solvent, yielding low recoveries.

The product distribution achieved from the thermal and catalytic quinoline reactions are given in Table 2. The PMH and PHDN terms are good indicators of HYD activity and HDN selectivity. Precipitated RuS₂ and supported NiMo/Al₂O₃ showed the highest and nearly equivalent PMH of ~49%. Precipitated MoS₂ produced a PMH of ~42% and CoMo/Al₂O₃, 39%, while the other catalysts yielded lesser amounts of hydrogenation, ranging from 24 to 30% PMH. The catalysts can be ranked according to their ability to hydrogenate quinoline in terms of PMH: RuS₂-3 = NiMo/Al₂O₃ > MoS₂-3 = CoMo/Al₂O₃ > WS₂-2 = Cr₂S₃ -4 > FeS_x-2 > thermal. The number to the right of the sulfide indicates the batch number. Precipitated RuS₂ achieved the highest PHDN of 10.8%; NiMo/Al₂O₃ and precipitated MoS₂ achieved 8.9% and 8.0%, respectively. Likewise, RuS₂-3 and NiMo/Al₂O₃ also gave the highest PHYG, but, in this case, RuS₂ with a PHYG of 17.3% was substantially more effective than NiMo/Al₂O₃ at 10.2%. The remaining catalysts and the thermal reaction showed no denitrogenation and little hydrogenolysis.

A comparison of the precipitated transition metal sulfides to their commercial or mineralogical analogues is given in Table 3. Commercial RuS₂ was not available. Only in the case of WS₂ did the commercial metal sulfide give the same degree of HYD activity as the precipitated metal sulfide. For both MoS₂ and Cr₂S₃, the precipitated sulfide gave higher HYD activity and for MoS₂ higher PHDN and PHYG.

Table 3. Activity and Selectivity Comparison of Precipitated to Commercial Transition Metal Sulfides

Catalyst	PMH, %	PHDN, %	PHYG, %
None	5.0	0.0	0.0
Cr ₂ S ₃ -4	28.8	0.0	0.0
Cr ₂ S ₃ -C	25.9	0.0	3.1
MoS ₂ -3	41.7	8.0	10.4
MoS ₂ -C	29.4	0.0	1.7
WS ₂ -2	30.9	0.4	2.4
WS ₂ -C	32.9	0.0	2.5

Since NiMo/Al₂O₃ and precipitated RuS₂ gave comparable PMH of quinoline, the

Table 2

Product Distribution from Thermal and Catalytic Quinoline Reactions

Type Catalyst	None	Cr ₂ S ₃ -4	MoS ₂ -3	WS ₂ -2	FeSx-2	RuS ₂ -3	CoMo/Al ₂ O ₃	NiMo/Al ₂ O ₃
MoleNH ₃ x 100%								
Mole Q1	2.8	0.2+0.1	2.8+1.5	0.34+0.48	0+0	0.42+(-)		1.06+1.4
Mole% CH ₄	0	0+0	0	0+0	0+0	0+(-)		0.004+0.006
H ₂ consumption, %	7.7	1.5+4.9	11.8+6.9	-7.1+7.1	3.3+15.6	18.1+(-)		13.1+18.6
M Q C	0+0	0+0	1.6+0.2	0.2+0	0+0	7.7+1.0	0.5+0.0	4.1+0.4
o u h	0+0	0+0	6.4+0.0	0.2+0.1	0+0	3.1+0.2	1.9+0.1	4.9+0.2
l i a	0+0	0.6+0.5	19.7+1.1	4.8+0.1	0.5+0.1	26.8+0.4	19.9+0.8	32.1+2.6
e n r	0+0	0.3+0.4	4.6+0.4	1.0+0.1	0.6+0.1	4.8+1.6	4.2+0.1	7.0+1.0
o g	0.2+0.3	1.2+1.1	2.4+0.7	0.5+0.1	1.4+0	1.8+0.2	1.2+0.1	3.3+0.8
% l e	0+0	3.1+0.1	2.4+0.1	0.9+0	0+0	6.5+0.4	1.3+0.2	1.3+0.1
i d	82.7+3.3	2.2+0.3	2.0+0.6	1.7+0	16.2+5.6	1.0+0	1.6+0.0	1.2+0.4
e	17.1+3.0	92.7+1.6	61.6+0.3	90.8+5.6	81.7+5.6	48.6+3.0	69.6+0.9	46.4+2.6
PMH, %	5.0+0.9	28.8+0.5	41.7+1.0	30.9+0.1	24.5+1.6	49.1+1.4	39.0+0.3	49.5+1.8
PHDN, %	0+0	0+0	8.0+0.2	0.4+0.1	0+0	10.8+1.2	2.4+0.1	8.9+0.1
PRB, %	0+0	3.1+0.1	10.4+0.1	1.3+0.1	0+0	17.3+1.6	3.7+0.4	10.2+0.0
Recovery, %	90.4+1.6	83.6+5.7	75.5+18.9	88.2+1.6	86.2+6.8	89.5+1.6	89.1+5.1	79.1+15.3

Compounds:

Reaction Conditions:

Time	30 min	PCH	propylcyclohexane
Temperature	380°C	PB	propylbenzene
Agitation Rate	850 cpm	DHQ	decahydroquinoline
H ₂ Charged Cold	1250 psig	CHP	2,3-cyclohexenopyridine
Reactant	2 wt% quinoline in hexadecane	PA	o-propylaniline
Reactor	15 cc microreactor	Q	quinoline
Catalyst Charge	~5.10 x 10 ⁻³ g catalyst g reaction mixture	THQ	1,2,3,4-tetrahydroquinoline

catalytic activity and selectivity of these two catalysts were tested with two individual products from quinoline hydrogenation: 1,2,3,4- tetrahydroquinoline (THQ) and 2-propylaniline (PA). The two catalysts achieved similar PMH and PHDN of THQ. NiMo/Al₂O₃ yielded more cis and trans decahydroquinoline (DHQ) than RuS₂ which produced more PA and nearly twice as much PHYG. When PA was used as the reactant, more hydrogenation and denitrogenation of PA was achieved with NiMo/Al₂O₃ than RuS₂. The lesser ability of RuS₂ to convert PA may explain the larger amount of PA observed in the THQ reaction with RuS₂.

Table 4. Catalytic Activity of NiMo/Al₂O₃ and RuS₂ in Several Reactant Systems

Catalytic Activity with THQ as a Reactant			
	<u>Thermal</u>	<u>NiMo/Al₂O₃</u>	<u>RuS₂</u>
PMH of THQ, %	0.7	27.8	25.4
PHDN, %	0.0	7.4	8.9
PHYG, %	0.0	8.5	14.6
Catalytic Activity with Propylaniline as Reactant			
PMH of PA, %	0.0	68.5	30.1
PHDN, %	0.0	81.4	36.5
Catalytic Activity with Propylaniline and Quinoline as Reactants			
PMH of PA, %		27.1	22.6
PHDN, %		35.6	27.1

To simulate the quinoline reaction system, 0.2 wt % quinoline was added to the PA solution (2 wt %). Quinoline served as a leveler of catalytic activity. The NiMo/Al₂O₃ was severely poisoned resulting in substantial reductions in both the HYD and HDN ability of NiMo/Al₂O₃ while RuS₂ was affected to a lesser extent showing a one-third reduction in PMH and PHDN. Thus, the presence of basic nitrogen in quinoline and THQ reduced the inherent activity of NiMo/Al₂O₃ to make NiMo/Al₂O₃ effectively equivalent to RuS₂ in both activity and selectivity in the quinoline system.

Recently, a catalyst containing 40% reduced Pt on silica has been shown to be an active HDN catalyst (7). The HDN ability of Pt/SiO₂ in the quinoline model system was investigated at temperatures ranging from 200 to 380°C as shown in Table 5. At 200°C, Pt/SiO₂ achieved the same activity as Cr₂S₃ and WS₂ at 380°C, with a PMH of ~35%. The activity of Pt/SiO₂ increased with temperature up to 340°C yielding 71% PMH and 9.8% PHDN; the PHDN was similar to that of RuS₂ with Pt/SiO₂ at 380°C. None of the products from the quinoline reaction pathway was observed; only higher boiling compounds were present. Even the solvent hexadecane was no longer present.

Table 5. Effect of Temperature on Activity of Pt/SiO₂ for Quinoline Hydrodenitrogenation

Temperature, °C	200	250	300	320	340	380
M Q C PCH	0	0	1.9	3.4	9.7	0
o u h PB	0	0	0	0	0.1	0
l i a DHQc	9.7	47.4	64.6	61.6	70.7	0
e n r DGQc	5.1	9.1	10.4	10.4	12.6	0
o g CHP	3.5	0.8	1.2	1.2	0.9	0
% l e PA	0	0	0	0	0.4	0
i d Q	0.9	1.0	0	0	0	0
n THQ	80.8	39.8	22.1	23.4	5.5	0
e						
PMH, %	34.0	53.4	62.1	61.8	71.3	-
PHDN, %	0	0	1.9	3.4	9.8	-
PHYG, %	0	0	1.9	3.4	10.2	-
Recovery, %	91.1	93.6	80.9	93.1	93.1	75.5

A comparison of the activity and selectivity of Pt/SiO₂, PtS₂ obtained from Alfa Chemicals and precipitated RuS₂ is given in Table 6. At 250°C, a temperature where Pt/SiO₂ showed considerable activity, PMH values of RuS₂ and PtS₂ showed equivalent HYD activity, ~29 to 30%, while Pt/SiO₂ showed considerably more, ~53%. None of the catalysts was able to denitrogenate quinoline and almost no hydrogenolysis occurred at this temperature.

Table 6. Comparison of the Activity and Selectivity of PtS₂, Pt/SiO₂ and RuS₂ in the Quinoline Model System at 250°C

Catalyst	PtS ₂ -C	Pt/SiO ₂ -1	RuS ₂
PMH, %	29.1	53.4	29.8
PHDN, %	0.0	0.0	0.0
PHYG, %	0.0	0.0	0.1

Coal Liquefaction Reactions. Two precipitated transition metal sulfides, RuS₂ and MoS₂, rivaled the commercial hydrotreating catalysts, NiMo/Al₂O₃ and CoMo/Al₂O₃, respectively, in their ability to hydrogenate and denitrogenate quinoline. Thus, RuS₂, MoS₂, NiMo/Al₂O₃ and Pt/SiO₂ were chosen as catalysts in coal liquefaction reactions to evaluate their efficiency in hydrogenating and removing nitrogen from coal.

Anthracene was used as the solvent for the coal liquefaction reactions. Since anthracene readily cracks under catalytic hydrogenation conditions (8), some hydrocracked products were expected; however, the presence of nitrogen heterocycles in the coal system moderated catalyst activity and reduced the amount of anthracene hydrocracking. For some of the reactions, the total anthracene products, including both hydrogenated and hydrocracked species, were measured, accounting for a 97 to 101% recovery of anthracene in thermal reactions and in reactions using NiMo/Al₂O₃ and RuS₂. However, when Pt/SiO₂ was used, only 74% recovery of the anthracene was achieved. With quinoline Pt/SiO₂ showed the production of high molecular weight materials at 380°C; this same phenomenon may have occurred in the coal reactions at the lower reaction temperature of 340°C.

The product distributions obtained from thermal and catalytic liquefaction reactions are given in Table 7. The reactions performed at 425°C yielded nearly equivalent coal conversions ranging from 94.5% for the thermal reaction to 99.0% for the reaction with RuS₂. The amount of light hydrocarbon gases produced was almost constant for all of the reactions yielding 15% for MoS₂ and RuS₂ and 14% for NiMo/Al₂O₃ while the thermal reaction produced nearly 19%. Therefore, the liquid products produced were quite similar in all reactions, ranging from 75.8% for the thermal reaction to 83.3% for RuS₂-5, thereby, providing a nearly equivalent basis for directly comparing the products from different reactions.

Comparing the product distributions, the sum of the polyfunctional compounds and THFS decreased from 20.5% for the thermal case to 9.0% for MoS₂-5&7, 6.4% for RuS₂-5 and 6.7% with NiMo/Al₂O₃. The total amount of product soluble in MCM increased by more than 10% in the catalytic compared to the thermal reactions. Considerably more of the heavier fractions was upgraded in the catalytic reactions producing a higher percentage of the products in the hydrocarbon (HC), nitrogen heterocycle (NH), and hydroxylaromatic (HA) fractions. In Figure 2, the product fractions produced from the different reactions are plotted against the catalyst specific surface area. The HC fraction produced followed the catalyst specific area: 17% for no catalyst, 34% for MoS₂-5&7, 49% for RuS₂-5 and 59% for NiMo/Al₂O₃. A maximum in Figure 2 is observed in the amount of NH produced, starting at 14% in the thermal reaction reaching ~19.5 and 18.2% with MoS₂-5&7 and RuS₂, respectively, and decreasing to ~11.0% with NiMo/Al₂O₃. Compared to the thermal reaction, the HA fraction decreased in the presence of the catalysts according to their specific surface area. Thus, the increased solubility of the coal-derived material in the MoS₂-5&7 and RuS₂ reactions was directly reflected in an increase in the NH and HC fractions since both the PC and HA fractions decreased. NiMo/Al₂O₃, attaining lower NH and higher HC fractions than the transition metal sulfides, performed better as a HDN catalyst than did RuS₂ in the coal

system.

Table 7. Product Distribution of Coal Liquefaction Reactions at 425°C

Type Catalyst	None	MoS ₂ -567	RuS ₂ -5	NiMo/Al ₂ O ₃
Surface Area, m ² /g	-	24.1	81.5	174
g cat/g reactant	0.20	0.20	0.20	0.20
Temperature, °C	425	425	425	425
H ₂ Consumption, %	6.2	8.5	14.2	15.3
Recovery, %	95.3	91.8	92.2	89.3
Coal Batch	A	A & B	B	B
M GAS	18.61	15.16	15.61	13.76
A M HC	17.02	34.08	48.83	58.80
F C NH	13.99	19.47	18.20	11.02
W M HA	24.36	20.11	10.33	6.74
t C S PC	9.70	2.98	0.61	1.82
O Total MCMS	65.07	76.64	77.97	78.37
% A THFS	10.78	6.01	5.83	4.85
L PC+THFS	20.48	8.99	6.44	6.67
IOM	5.54	2.19	1.05	3.04
Conversion, %	94.46	97.81	98.95	96.95
M A c DHA	16.11	13.36	4.00	2.17
o N h OHA	9.83	26.88	60.23	53.04
l T a HHA	58.43	38.26	17.97	16.30
e H r ANTH	2.61	0.20	0.0	0.0
g Total	86.97	79.05	80.49	71.51
% e CRS	96.96	-	101.91	100.55
d				

The anthracene hydrogenation products from the liquefaction reactions are plotted versus catalyst specific surface area in Figure 3. Anthracene is sequentially hydrogenated from anthracene to DHA to HHA to OHA, which then hydrocracks to lighter products. In the thermal reaction, 2.6% anthracene remained unconverted; this amount decreased rapidly below GC detectability limits under catalytic conditions. DHA and HHA were at a maximum in the thermal reaction and decreased as catalysts with increasing surface areas were used, while OHA showed a maximum at an intermediate catalyst surface area. Both the OHA maximum and decrease in the sum of the anthracene hydrogenation products were due to hydrocracking of OHA. The CRS of the anthracene products in Table 7 indicates that all the anthracene could be accounted for in hydrogenated and hydrocracked products.

Coal liquefaction reactions using Pt/SiO₂ employed two stage processing in which a thermal reaction at 425°C was performed to convert most of the coal, followed by an hour reaction at 340°C with Pt/SiO₂. The two stage reaction scheme was used to dissolve the coal in the first stage and possibly upgrade and eliminate some of the potential catalyst poisons before introduction of the catalyst. The Pt/SiO₂ did not produce either a satisfactory or a reproducible suite of products. High gas makes of ~34% were observed along with substantial losses in the HC fraction. The THFS amount was quite large ~38% compared to ~5 for the transition metal sulfides. Analysis of the anthracene solvent accounted for only ~74% of the original anthracene charged to the reactor, indicating production of higher molecular weight compounds as in the quinoline reaction.

Summary

Two precipitated transition metal sulfides MoS₂ and RuS₂ possessed both HYD activity and HDN selectivity in the quinoline model system. These transition metal sulfides rivaled the commercial hydrotreating catalysts in activity; RuS₂ was comparable to NiMo/Al₂O₃ and MoS₂ to CoMo/Al₂O₃. NiMo/Al₂O₃ possessed higher activity for PA hydrogenation than did RuS₂; however, RuS₂ was not as severely

poisoned by quinoline as NiMo/Al₂O₃. Pt/SiO₂ at 340°C was as active a catalyst for quinoline HDN as NiMo/Al₂O₃ at 380°C. Both precipitated MoS₂ and RuS₂ achieved upgrading in coal liquefaction reactions showing HYD activity; however, the higher surface area NiMo/Al₂O₃ showed greater HYD activity and considerably more nitrogen removal. Pt/SiO₂ was readily poisoned in the coal system and was not effective for coal HDN.

Table 8. Products from Two Stage Liquefaction Using Pt/SiO₂

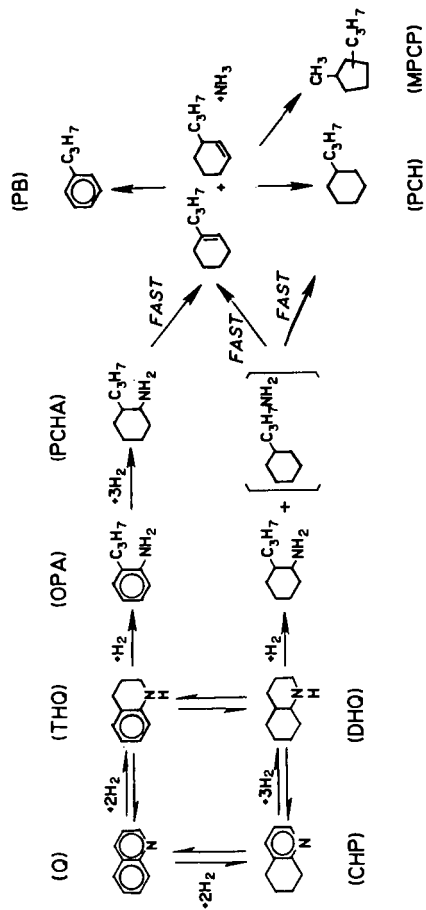
Catalyst Loading		H ₂ Consumption, %	
g cat/g reactant		Recovery, %	
Temperature, °C		Coal Batch	
(first stage/second stage)			
0.20		1.65 ± 2.33	
425/340		111.74 ± 12.95	
		B	
M GAS	33.81 ± 7.15	M A c DHA	4.48 ± 0.78
A M H	-9.57 ± 11.96	o N h OHA	40.92 ± 1.82
F C NH	19.13 ± 3.85	l T a HHA	14.79 ± 1.90
W M HA	24.09 ± 1.08	e H r ANTH	0.0 ± 0.0
t C S PC	4.95 ± 0.81	g Total	60.18 ± 4.50
O Total MCMS	38.95 ± 16.09	% e CRS	73.97 ± 10.85
% A THFS	33.29 ± 17.92	d	
L PC+THFS	38.24 ± 18.72		
IOM	-5.69 ± 8.97		
Conversion	105.69 ± 8.97		

Acknowledgements

The authors gratefully acknowledge the support of this work by the Department of Energy under Contract No. DEAC22-83PC60044.

References

- Chianelli, R.R., Dines, M.B., Inorg. Chem., **17**(10), 2758(1978).
- Pecoraro, T.A., Chianelli, R.R., J. Catal., **67**, 430-445 (1981).
- Boduszynski, M.M., Hurtubise, R.J., Silver, H.F., Anal. Chem., **54**, 375-381 (1982).
- Satterfield, C.N., Modell, M., Hites, R.A., Declerck, C.J., Ind. Eng. Chem. Process Des. Dev., **17**(2), 141 (1978).
- Satterfield, C.N., Cocchetto, J.F., Ind. Eng. Chem. Process Des. Dev., **20**, 53 (1981).
- Satterfield, C.N., Yang, S.H., Ind. Eng. Chem. Process Des. Dev., **23**, 11 (1984).
- Guttieri, M.J., Maier, W.F., J. Org. Chem., **49**, 2875 (1984).
- Weisser, O. and Landa, S., "Sulphide Catalysts, Their Properties and Applications," Pergamon Press, New York, 1973.



Q - quinoline
 THQ - 1,2,3,4 -tetrahydroquinoline
 CHP - 2,3 - cyclohexenopyridine
 DHO - decahydroquinoline (cis and trans isomers)
 OPA - o-propylaniline
 PCHA - propylcyclohexylamine
 PB - propylbenzene
 PCHE - propylcyclohexene (1,1 or 1,3)
 PCH - propylcyclohexane
 MPCP - methylpropylcyclopentane

Figure 1. Reaction Network.

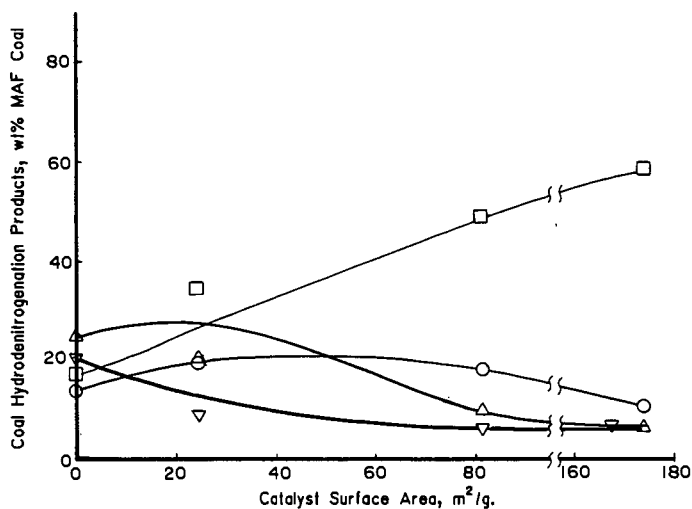


Figure 2. Effect of Catalyst Surface Area on Coal Hydrodenitrogenation Products: □-Hydrocarbons, ○-Nitrogen Heterocycles, △-Hydroxyl Aromatics, ▽-Polyfunctional Compound plus THF solubles.

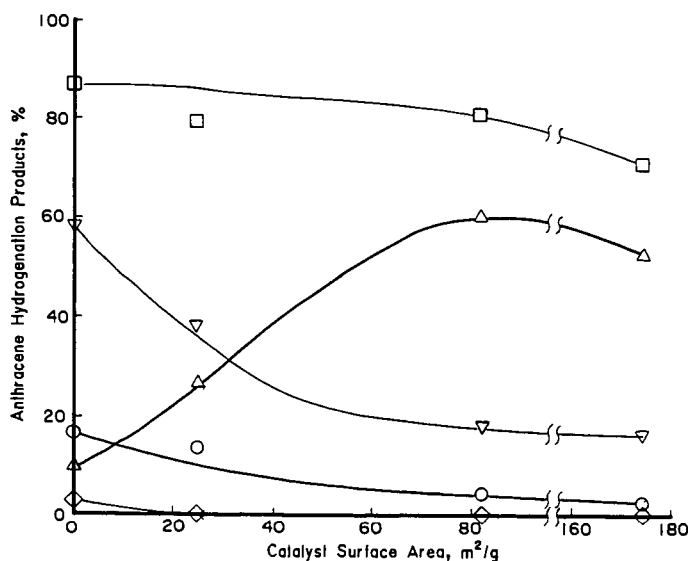


Figure 3. Effect of Catalyst Surface Area on Hydrogenation of Anthracene: ○-DHA, △-OHA, ▽-HHA, ◇-ANTH, □-Sum.

SAND87-0270C

CAUSES OF CATALYST DEACTIVATION DURING
QUINOLINE HYDRODENITROGENATION*

Frances V. Stohl

Sandia National Laboratories Albuquerque, NM 87185

Introduction

Previous studies (1,2) of catalyst samples from the Wilsonville Advanced Coal Liquefaction R&D Facility have shown that the initial rapid catalyst deactivation was due to the buildup of carbonaceous deposits on the catalyst. Greater than 75% of the catalyst's hydrogenation (HYD) activity was lost as soon as coal processing began (2). Variations in the amount of carbonaceous deposits (1) on the catalysts from several different Wilsonville runs, which used two different coals and three process configurations, were due to the process configuration but not the coal type. The heaviest hydrotreater feed (from the Reconfigured Integrated Two-Stage Liquefaction configuration) in the Wilsonville runs, yielded the most accumulation of carbonaceous deposits on the catalyst and therefore the greatest deactivation (1). Hydrotreating this feed resulted in an initial 67% loss of hydrodesulfurization (HDS) activity; hydrotreating the lightest feed (from the Double Integrated Two-Stage Liquefaction configuration) yielded only a 47% decrease in HDS activity.

As a result of the work on Wilsonville catalysts, a program has been initiated to identify the hydrotreater feed components that are most harmful to the catalyst. Previous studies (3) to determine the impacts of the various chemical classes of compounds found in a hydrotreater feed on catalyst activity showed that the aliphatic and neutral polycyclic aromatic compounds yielded much less deactivation than the total hydrotreater feed and the nitrogen polycyclic aromatic compounds (N-PAC) and hydroxy polycyclic aromatic hydrocarbons (HPAH) yielded much greater deactivation. The N-PAC yielded a 95% loss of extrudate activity with 98% of the active sites poisoned. The activity losses for all of these fractions were due to poisoning of active sites and decreased effective diffusivities. Chemical analyses of the HPAH and N-PAC fractions showed that both contained significant amounts of oxygen and nitrogen so that the individual effects of the nitrogen and oxygen compounds could not be separated. Therefore, additional studies (4) were performed using both nitrogen and hydroxy model compounds. Hydrotreating phenol and 1-naphthol yielded only about 35% losses in extrudate activity. Hydrotreating indole, a weak basic pyrrolic nitrogen compound, yielded a 50% loss and carbazole, a neutral pyrrolic compound, yielded a 24% loss. In contrast, pyridinic nitrogen compounds (pyridine, quinoline, acridine) yielded about 75% losses. These results showed that the strong basic nitrogen compounds are most harmful to the catalyst.

The current work involves determining the causes of deactivation due to hydrotreating pyridinic compounds. Quinoline was chosen as the model compound for this study because it represents a type of nitrogen compound present in coal-derived materials, and a hydrodenitrogenation (HDN) reaction network has been proposed for

* This work supported by the U.S. Dept. of Energy at Sandia National Laboratories under Contract DE-AC04-76DP00789.

this compound (5,6). In the proposed reaction scheme, at low temperatures, quinoline is hydrogenated to 1,2,3,4-tetrahydroquinoline (PyTHQ). PyTHQ is cracked to o-propylaniline (OPA), and then the nitrogen is removed, as ammonia, to give propylbenzene (PBz). At high temperatures, the hydrogenation of quinoline to 5,6,7,8-tetrahydroquinoline (BzTHQ) also becomes important. BzTHQ is further hydrogenated to decahydroquinoline (DHQ), which is then cracked and denitrogenated to yield mostly propylcyclohexane (PCH). PyTHQ can also be hydrogenated to DHQ and OPA can also be hydrogenated and denitrogenated to PCH.

The initial work reported here on the causes of deactivation due to hydrogenating quinoline will cover the impact of process conditions on deactivation and the determination of the effects of the reaction scheme intermediates and products on deactivation.

Experimental Procedures

Quinoline was hydrogenated under a variety of conditions to determine the effects of process variables on catalyst deactivation. In addition, each of the intermediates formed during quinoline HDN was catalytically hydrotreated and the resultant deactivation measured. The aged catalysts were characterized and the intermediate compounds and products reported for the HDN reaction scheme (5) were quantified.

Materials

The catalyst was Shell 324M with 12.4 wt% Mo and 2.8 wt% Ni on an alumina support in the form of extrudates measuring about 0.8 mm in diameter and 4 mm in length. Prior to use the catalyst was presulfided with a 10 mol% H₂S in H₂ mixture at 400°C and atmospheric pressure for 2 hours. The structures of the model compounds used in this study are shown in Table 1.

Hydrotreating Experiments

Each hydrotreating experiment was performed in 26 cc batch microreactors with 1200 psig H₂, cold charge pressure. Runs were made for either 5 minutes or 120 minutes at either 300°C or 400°C. Unless otherwise stated, experiments were performed with 1.5g of model compound and 0.5g presulfided catalyst. The aged catalysts were Soxhlet extracted with tetrahydrofuran prior to activity testing. Elemental analyses were performed on the extracted aged catalysts.

Activity Testing

Hydrogenation activities of fresh and aged catalysts were determined by measuring the rate of hydrogenation of pyrene to dihydropyrene in 26 cc microreactors at 300°C with 450 psig H₂, cold charge pressure (7). Experiments with whole extrudates and catalyst ground to -200 mesh enabled determination of the losses of extrudate and intrinsic activities (8) respectively. Loss of intrinsic activity is proportional to the loss of active sites.

Liquid Product Analyses

Intermediates and products reported for the quinoline HDN reaction network (5) were identified using GC/MS and quantified using GC analysis with commercially available compounds as standards.

Results and Discussion

Activity Testing

The measured extrudate and intrinsic activity losses for the runs with quinoline at 300°C and 400°C for 5 minutes and 120 minutes are given in Table 2. The catalysts from all these runs had extrudate activity losses ranging from 73 to 84% and intrinsic activity losses from 85 to 94%. The differences in the measured extrudate activities of the catalysts from the two times at a given temperature are not significant. However, the catalyst from the 400°C run for 120 minutes is slightly more deactivated than the catalyst from the 300°C run for 5 minutes. The intrinsic activity losses for the catalysts from the quinoline runs are all the same within experimental error. These results show that deactivation occurs very rapidly and that significant changes in time and temperature have little effect on the extent of deactivation.

Effects of variations in the catalyst to reactant ratio were tested using quinoline at 300°C for 120 minutes. A run with a 1:1 ratio yielded a 64% extrudate activity loss, whereas runs with 1:3 and 1:9 ratios gave 76% and 77% losses respectively. These results suggest that a higher catalyst to quinoline ratio yields less deactivation, which is probably due to the greater number of active sites relative to the amount of deactivating compound.

The four intermediate compounds (PyTHQ, OPA, BzTHQ, DHQ) and the two products (PBz, PCH) were each hydrotreated with catalyst at 300°C for 5 minutes and 120 minutes. The measured extrudate and intrinsic activity losses are given in Table 3. The results show that for the 5 minute runs, the three hydrogenated species (PyTHQ, BzTHQ, DHQ) yielded comparable deactivation (about 70% extrudate activity loss) to hydrotreating quinoline. For the 120 minute runs, quinoline, DHQ, and BzTHQ yielded comparable activity losses to the 5 minute runs; PyTHQ yielded significantly less deactivation (53%). With both run times, OPA caused less deactivation than the other intermediates and PCH caused the least deactivation. PBz caused deactivation by a different mechanism than quinoline, PCH or the intermediates as indicated by the low amount of active sites poisoned. The 52% extrudate activity loss caused by PBz may be due to diffusional limitations caused by the deposition of carbonaceous material in the outer regions of the catalyst. This is a different mechanism than observed for quinoline so that this compound is not important in quinoline deactivation. The results of the hydrotreating experiments with the intermediate compounds and products indicate that greater deactivation is correlated with the hydrogenated intermediates (PyTHQ, BzTHQ and DHQ) and quinoline. It is not known why PyTHQ causes less deactivation at the longer time; it may be due to the greater reaction of PyTHQ at the longer time (see below).

Elemental Analyses of the Catalysts

There is a correlation between the carbon contents of the aged catalysts (Table 4) and deactivation. Quinoline, PyTHQ, BzTHQ and DHQ caused the most deactivation and gave the highest carbon contents. PCH yielded the least deactivation and gave the lowest carbon content. However, it appears that above a certain carbon content, when the catalyst is significantly deactivated, additional carbonaceous deposits do not have much effect on activity. For example, aged catalyst from the 120 minute run with quinoline at 300°C has about a 30% higher carbon content than the catalyst from the 5 minute run and yet they both are equally deactivated.

Liquid Product Analyses

Quantitative analyses of the liquid products from the quinoline runs performed at 300°C and 400°C for 5 minutes and 120 minutes are given in Figure 1. The amount of unidentified components (components that are not intermediates or products in the reported quinoline HDN reaction scheme (5)) is equal to 100% minus the height of the bar. The quantity of unidentified compounds increased with both time and temperature. At 300°C for 5 minutes, 19% of the liquid product was unidentified whereas at 400°C for 120 minutes 86% was unidentified. These results indicate that side reactions occur to a greater extent under more severe reaction conditions. The product distribution for the 300°C run for 5 minutes also shows that the hydrogenation of quinoline to PyTHQ was very rapid. Increasing time and/or temperature yielded more OPA. None of these runs yielded significant concentrations of PBz or PCH. The 400°C run products show a higher concentration of BzTHQ than the 300°C runs in agreement with previous results (5).

The product distributions for the run with a 1:1 quinoline to catalyst ratio had 54% unidentified product, whereas the runs with 1:3 and 1:9 ratios had 44% and 24% respectively. Therefore, a higher catalyst to quinoline ratio yields more side reactions. The product distributions also showed increasing concentrations of OPA and PCH with increasing catalyst to quinoline ratios.

The product distributions for the 5 minute runs with the intermediates and products showed no significant amount of unidentified material. In addition, the only significant reaction that occurred in any of these runs was the hydrogenation of BzTHQ to about 15 wt% DHQ. In the 120 minute runs (Figure 2), PyTHQ, DHQ and BzTHQ yielded 29%, 19% and 9% unidentified product respectively. In addition, PyTHQ formed more OPA, DHQ and PCH. OPA yielded more PCH. PBz was hydrogenated to a significant amount of PCH, and BzTHQ was hydrogenated to DHQ.

There is no correlation between the amount of deactivation and the amount of unidentified material in the liquid product. This is shown by the results of the quinoline runs in Table 2 and Figure 1. In addition, the 1:1 catalyst to quinoline run yields less deactivation than the 1:3 run, but yields more unidentified material.

The rapid deactivation due to hydrotreating quinoline and the hydrogenated heterocyclic intermediates may be due to the low reaction rates of the intermediate compounds to denitrogenated products at 300°C. Some of the intermediates (PyTHQ and DHQ) are strong basic compounds (9). Therefore, these compounds would be strongly adsorbed on the catalytic sites causing site blockage. Additional studies are underway to evaluate the effects of hydrotreating the intermediates and products at 400°C and to characterize the deposits on the aged catalysts.

References

1. Stohl, F.V. and Stephens, H.P. submitted to I&EC Research.
2. Stephens, H.P. and Stohl, F.V. ACS Division of Petroleum Chemistry Preprints 30(3), 465, 1985.
3. Stohl, F.V. and Stephens, H.P. ACS Division of Fuel Chemistry Preprints 31(4), 251, 1986.
4. Stohl, F.V. Proc. Direct Liquefaction Contractors' Review Meeting, Oct. 20-22, 1986, Monroeville, PA.
5. Satterfield, C.N., Modell, M., Hites, R.A. and Declerck, C.J. Ind. Eng. Chem. Process Des. Dev. 17(2), 141, 1978.
6. Cocchetto, J.F. and Satterfield, C.N. Ind. Eng. Chem. Process Des. Dev. 20, 49, 1981.

7. Stephens, H.P. and Kottenstette, R.J. ACS Division of Fuel Chemistry Preprints 30(2), 345, 1985.
8. Stephens, H.P. and Stohl, F.V. ACS Division of Fuel Chemistry Preprints 29(6), 79, 1984.
9. Satterfield, C.N. and Cocchetto, J.F. Ind. Eng. Chem. Process Des. Dev. 20, 53, 1981.

Table 1. Model compounds.


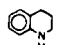
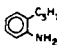
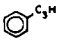
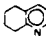
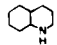
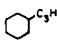
Quinoline	PyTHQ	OPA	PBz
			
BzTHQ	DHQ	PCH	
			

Table 2. Fraction of measured extrudate and intrinsic activity losses for the runs with quinoline. Results are relative to fresh presulfided catalyst.

TEMPERATURE (°C)	EXTRUDATE		INTRINSIC	
	5 min	120 min	5 min	120 min
300	0.73	0.76	0.89	0.89
400	0.80	0.84	0.85	0.94

Table 3. Fraction of measured extrudate and intrinsic activity losses for the 300°C runs with the intermediates and products. Results are relative to fresh presulfided catalyst.

REACTANT	EXTRUDATE		INTRINSIC	
	5 min	120 min	5 min	120 min
PyTHQ	0.70	0.53	0.85	0.80
OPA	0.54	0.47	0.66	0.66
PBz	0.52	0.53	0.22	0.27
BzTHQ	0.75	0.66	0.88	0.83
DHQ	0.68	0.67	0.82	0.78
PCH	0.14	0.21	0.37	0.35

Table 4. Carbon contents of the aged catalysts from the 300°C runs reported as weight percents.

	Quin	PyTHQ	OPA	PBz	BzTHQ	DHQ	PCH
5 min	4.81	4.25	3.86	2.28	5.19	4.07	1.81
120 min	6.36	NA*	3.43	2.49	4.76	4.19	1.99

* Not analyzed.

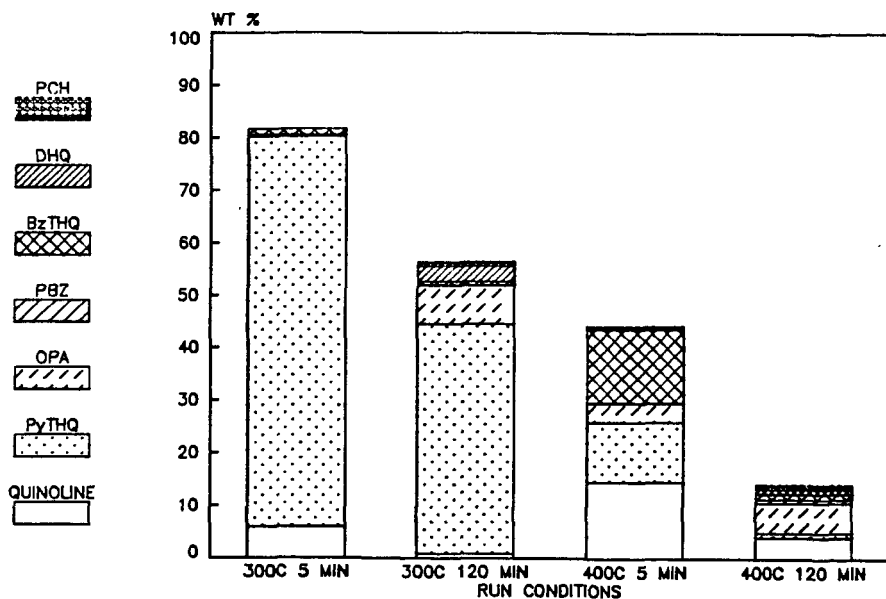


Figure 1. Liquid product analyses from the runs with quinoline.

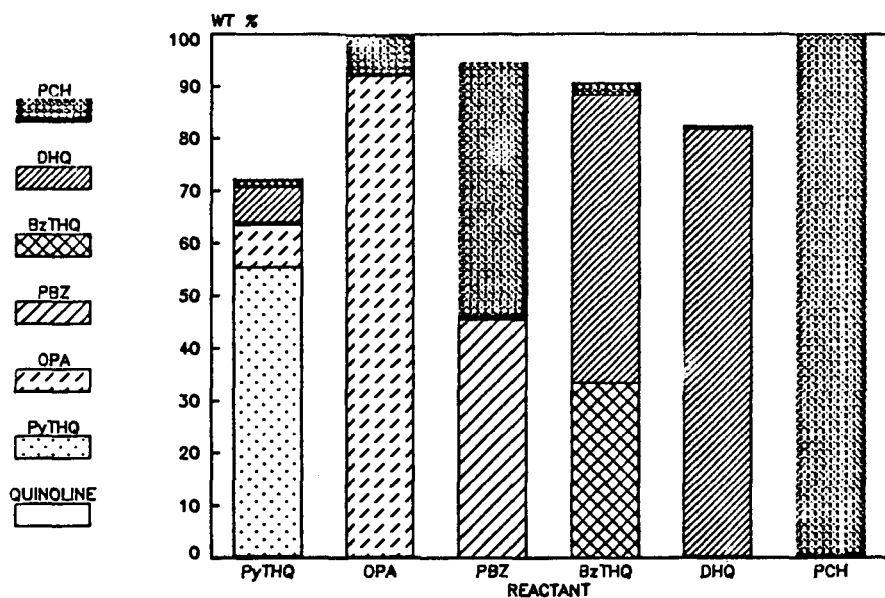


Figure 2. Liquid product analyses from the guns with the intermediates and products at 300°C for 120 minutes.

HYDROTREATMENT EFFECTS ON WILSONVILLE COAL LIQUIDS;
COMPUTER-ASSISTED EVALUATION OF MULTISOURCE ANALYTICAL DATA

Koli Taghizadeh, Rita Hardy, Robert Keogh, Jack Goodman, Burt Davis
Kentucky Energy Cabinet Laboratory, Lexington, KY 40512

Henk L.C. Meuzelaar
University of Utah, Biomaterials Profiling Center
Salt Lake City, Utah 84108

INTRODUCTION

As reported earlier (1), monitoring time-dependent changes in Wilsonville coal-derived liquid (CDL) streams by means of computer-assisted direct mass spectrometry (MS) techniques enables detection of process related trends in the relative concentration of CDL components. Notwithstanding the potentially high information yield of this MS procedure, additional data is required for unambiguous identification and interpretation of some of the more complex components or trends. In fact, the CDL's produced by the Wilsonville pilot plant are routinely analyzed by an extensive array of conventional tests, including elemental analysis and solubility classes, as well as by advanced chromatographic and/or spectroscopic techniques, e.g., proton nuclear magnetic resonance spectroscopy (NMR) and carbon-13 NMR.

Unfortunately, the sheer volume of the data produced by this broad array of tests during a 2 to 3 month run makes it very difficult to discern some of the more interesting trends and effects. In the experiments reported here computerized multivariate analysis techniques such as factor, discriminant and canonical correlation analysis, were used to remove redundant data or experimental noise and to highlight relevant components and trends.

EXPERIMENTAL

A schematic flow diagram of the Wilsonville Advanced Coal Liquefaction facility in the Integrated Two-Stage Liquefaction (ITSL) mode is shown in Figure 1. The feed to the second stage hydrotreater is a mixture of thermal distillate (450°F+) and Critical Solvent De-ashed Thermal Residue (CSD TR). The hydrotreater "atmospheric flashed bottoms" stream is recycled to the first stage dissolver. The temperature/time profile of the hydrotreater as well as a seven day average of the difference (ΔT) between the outlet and inlet temperature of dissolver are shown in Figure 2. The hydrotreater temperature was increased in 10°F increments from 720°F to 740°F as the catalyst aged. However, as shown in Figure 2, several times during the run, operator responses to technical problems caused the actual hydrotreater temperature to be much lower than the set temperature. It is intended that the dissolver temperature be controlled primarily by the temperature of the preheated coal slurry, which flows from a preheater into the dissolver.

The data presented here were generated for samples collected during run No. 244 at the Wilsonville pilot plant when they were processing an Illinois No. 6 coal from a Burning Star mine. The average composition of the coal was: proximate analysis - VM 36%, FC 50%, moist. 4%, ash 10%; ultimate analysis - C 68.2%, H 4.5%, N 1.2%, S 3.3, mineral matter 10.6%, O (diff.) 12.2%. The sampling points for both hydrotreater feed and hydrotreater product (atmospheric flashed bottoms) samples are shown in Figure 1 and the days on which samples were collected are indicated in Figure 2. For consistency with earlier work (1), that numbering system was retained; unfortunately, the NMR and conventional data were not available for sample nos. 2, 3, 4, 12, 13 and 14. Therefore these samples were omitted from this data set.

Elemental carbon, hydrogen and nitrogen values were obtained using a LECO CHN-600 analyzer (2). Direct oxygen determinations were obtained by a modified Untera-zucher method (3), and sulfur determinations were made on a LECO SC-132 instrument (4). The solubility class (oils, asphaltenes, preasphaltenes) and phenols determinations were described in detail elsewhere (5,6). Vacuum distillations utilized a modified ASTM D-1160 apparatus that was maintained at approximately 0.1 mmHg during the distillation. Following standard practice, the distillation was considered to be complete when cracking became noticeable.

Proton NMR samples were prepared by diluting approximately 0.25 g of the CDL with 0.25 ml of CDCl_3 which was doped with 1 wt. % TMS (tetramethyl silane). Spectra were recorded on a Varian EM-390 instrument. A minimum of two integrations were recorded for the proton regions determined. The proton spectra were divided into seven regions which correspond to different proton type resonances (7). Samples for carbon 13-NMR were prepared by diluting 1.5 g of the CDL with 1.0 ml of CDCl_3 . Five mg of $\text{Cr}[\text{acac}]_3$ was added as a relaxation agent. Spectra were recorded with a Varian FT-80 spectrometer over a 4000 Hz spectral window at 20 MHz. Integrals were obtained in duplicate. The carbon 13-NMR spectra were divided into an aliphatic (0-50 ppm) and an aromatic region (100-200 ppm) (8).

Solutions for low voltage MS were prepared as follows: about 2 mg of each CDL were weighed and dissolved in 1 ml of a 1:1 benzene:methanol mixture. Solutions were stored at -10 °C prior to analysis. Low voltage MS were obtained using an Extranuclear 5000-1 quadrupole system under the following conditions: temperature rise time 5.5 s, equilibrium temperature 610 °C, total heating time 10 s, electron energy setting 12 eV, mass range scanned m/z 20-260, scanning rate 1000 amu/s, total scan time 20 s. Each sample was analyzed in triplicate and the resulting spectra were normalized using the SIGMA program package (9).

Data analysis was performed using factor analysis and canonical correlation analysis procedures, described elsewhere in more detail (10,11 and 12). Canonical correlation analysis was used to compare two data sets, e.g., on the basis of factor scores. The canonical correlation technique constructs sets of linear combinations of the variables in the two data sets in such a way that the first linear combination (canonical variate function) for the first data set and the first linear combination of the second data set show maximum correlation. The second set of linear combinations describes the maximum correlation remaining in the data set and so on.

RESULTS AND DISCUSSION

Figure 3 shows the averaged low voltage mass spectra of the hydrotreater feed and hydrotreater product (flushed bottoms). The hydrotreater feed spectrum shows relatively prominent peak series at m/z 168, 182, 196, 210 and 224, tentatively identified as acenaphthenes and/or biphenyls with various of alkylsubstitution. The hydrotreater product spectrum shows major peak series at m/z 172, 186, 200, 214, and 228; these are believed to represent hydroaromatic hydrocarbons such as octahydrophenanthrenes and/or hexahydrofluorenes with possible contributions from tetrahydroacenaphthenes.

Other homologous ion series at m/z 212, 226, 240, 254 in the hydrotreated product spectrum obviously represent decahydropyrenes and perhaps decahydrofluoranthenes. Although there is no direct way to identify the various mass peaks in Figure 3, all major compound series were tentatively identified by GC/MS as well as MS/MS analysis of selected samples and compounds as well as by comparisons with GC/MS literature data on Wilsonville CDL's (13,14). Close scrutiny of Figure 3 may raise the question why the main compound series observed in the hydrotreater product does not correspond directly to the main compound series in the hydrotreater feed? An obvious answer is that the hydroaromatic compounds formed during hydrotreatment are

substantially more volatile than the corresponding aromatic parent compound series. Consequently, many of these low boiling volatiles are removed in the atmospheric distillation overhead fraction (see Figure 1).

A second aspect which should be pointed out here is that the spectra in Figure 3 represent only the CDL components which were able to reach the ion source without preheating the MS inlet system. Consequently, compounds with about 5-rings and higher are not included in Figure 3. However, as established in a separate series of experiments (1) involving preheating of the MS inlet as well as comparisons with Field Ionization MS data obtained at SRI, differences seen in Figure 3 are quite characteristic and representative of the overall changes observed as a result of hydrotreatment even if these higher components had been volatilized. In other words, the changes observed for the 2-4 ring systems in Figure 3 were qualitatively similar to those observed in higher condensed compound series.

To enable more systematic comparisons among the spectra of all 14 samples, the low voltage MS data were subjected to factor analysis. Figure 4 shows the factor score plot of the first two factors, together explaining 74% of the total variance in the data. The hydrotreater feed (categories 1-10) and hydrotreater product (categories 11-20) samples form two distinct clusters. In fact, Factor I and Factor II, with 64.4% and 9.6% of total variance respectively, appear to reveal two major trends in the data set; namely a hydrotreatment effect (Factor I) and a time + temperature effect (Factor II, compare with the time + temperature trend in Figure 2). Factors I and II explained 74% of the total variance in the data whereas the remaining 26% was largely explained by factors 3-10, none of which revealed significant components or trends.

Conventional coal liquid characterization data as well as ^1H and ^{13}C NMR data obtained for both sets of samples are shown in Table I. The effects of hydrotreatment are immediately apparent upon inspection of many of the parameters in Table I. However, neither the time + temperature trend, observed in the low voltage MS data nor any of the other trends which might be present are readily discernible by visual examination of the multidimensional information in Table I. Consequently, multivariate statistical analysis techniques such as factor analysis, are needed to reduce the data and reveal the main underlying trends.

To obtain a better insight into the components and trends described by the NMR and conventional data, factor analysis was performed on this data set as well. Eight factors with eigenvalues >1.0 , together describing a total variance of 98.6% were obtained. The score plot of the first two factors is shown in Figure 5 with Factor I (57.4%) and Factor II (13.6%) revealing the hydrotreatment effect and time + temperature effect respectively. Again, the remaining factors (27.6%) did not reveal any clear trends or components. Encouraged by the obvious similarities between the information provided by Figures 4 and 5, we determined the degree of overlap between the two data sets by means of canonical correlation analysis.

Two major canonical correlation functions were found, CVI (can. corr. = 0.998) and CVII (can. corr. = 0.946). The integrated score plot of both data sets is shown in Figure 6. To reduce the complexity of the low voltage MS data, the average of each triplicate analysis was plotted. As expected, the same two important trends were observed with CVI showing the effect of hydrotreatment and CVII describing a combined time + temperature effect.

Figure 7 shows the absolute difference between the CVI scores of hydrotreated feed and hydrotreated products of low voltage MS and conventional and NMR data; this enables a more direct evaluation of the efficiency of the hydrotreatment process to be made. Apparently, the differences between the composition of the hydrotreater

feed and the hydrotreater product sample become somewhat less pronounced towards the end of the run, indicating a loss of hydrotreatment efficiency with time.

Finally, Figures 8 and 9 allow a more detailed chemical evaluation of the trends and components represented by CVI and CVII. The mathematically extracted mass spectra of CVI (hydrotreatment effect) and CVII (time + temperature effect) are shown in Figure 8. The positive components of the spectrum Figure 8a, representative of the hydrotreater feed, show prominent acenaphthene and/or biphenyl series at m/z 168, 182, 196, 210, and 224 (compare with Figure 3a) as well as naphthalene series at m/z 142, 156, 170, 184, and 198. The negative components show dominant hydroaromatic ion series at m/z 172, 186, 200, 214, and 228 as well as at m/z 212, 226, and 240 (also observed in Figure 3b).

Interpretation of the spectrum of the second canonical variate function in Figure 8b is less straightforward. Obviously, we are looking at a shift in the average molecular weight of the vacuum distillate fraction that is seen by the mass spectrometer. As discussed above, the upper limit of the vacuum distillate range is primarily determined by the inlet temperature of the mass spectrometer. Conversely, the lower limit of the distillation range must be primarily determined by the cut-off point of the atmospheric distillation following hydrotreatment. This cut-off point is likely to reflect the steadily increasing hydrotreater temperature shown in Figure 2. Consequently, the early samples tend to be richer in low MW components than the later samples obtained at higher hydrotreater temperatures. This appears to be reflected in the trend shown in Figure 8b. Whether Figure 8b also reflects the effect of catalyst aging, e.g. in the form of changes in qualitative composition is hard to decide due to the close correlation between time and temperature in the overall experimental design shown in Figure 2. Moreover, minor but definite changes in overall coal quality, e.g., as a result of storage and/or variations in mine output, could also have contributed to the observed trends, thereby further complicating attempts at unambiguous chemical interpretation. Obviously, if these effects are to be distinguished in future studies, the experimental design of the process conditions will need to be aimed at decoupling the effects of catalyst aging, reactor temperatures, distillation conditions and changes in feed coal composition.

The loadings (correlation coefficients) of the NMR and conventional variables on the first canonical variate function are shown in Figure 9a. Heteroatomic concentrations (N, S, O), asphaltene and benzene insolubles as well as the relative concentration of all condensed and noncondensed aromatic protons and aromatic carbon are higher in the hydrotreater feed than in the product samples. Conversely, %C, %H, oil yield, relative concentration of alkyl and cyclic protons ($^1\text{H-NMR}$) and aliphatic carbons (carbon $^{13}\text{-NMR}$) are, as expected, higher in the hydrotreater product (flashed bottoms).

Loadings of NMR and conventional data on CVII (Figure 9b) show that hydrotreater temperature (T), dissolver temperature (ΔT) and time (t) show a strong, positive correlation with CVII (negative portion). With increasing time and temperature, more hydrogen is present in the nondistillate fraction which could reflect decreased catalyst efficiency; that is, the hydrocracking activity decreases relative to the hydrogenation activity. Moreover, heteroatoms such as N and S are not removed as efficiently in the later days of the run. The fact that %O appears to be higher in the early days may well be due to phenols at m/z 136, 150, 164 or a pseudocorrelation caused by the normalization of %C, H, N, O to 100%. Also distillate yields are higher in early days, whereas the nondistillate portion increases in later days. $^1\text{H-NMR}$ data show higher alkyl beta and gamma protons in early days. The low voltage MS data in Figure 8b indicate that this might be due to the presence of highly substituted tetralins and phenols. Conversely, the $^1\text{H-NMR}$ data show that the relative concentration of cyclic alphas and some type of cyclic beta hydrogen increases in later days; the higher hydroaromatics in low

voltage MS (Figure 8b) could account for this. Overall, the time + temperature trend represented by CVII indicates a loss of catalyst efficiency accompanied by decreased distillate yield, increased aromaticity and ring condensation and a substantial increase in hydrogen in the nondistillate fraction.

A speculative interpretation of the latter observation has catalyst aging producing a more pronounced loss of bond cleavage activity than of hydrogenation efficiency, thus resulting in the formation of alicyclic structures which remain in the increasingly larger nondistillate fraction. Alternatively, one might hypothesize that a loss of efficiency in capping newly formed radicals leads to an increased condensation through regressive reactions.

ACKNOWLEDGEMENTS

This work was supported by the Commonwealth of Kentucky, Kentucky Energy Cabinet and DOE Contract No. DEFC22-85PC80009 as part of the Consortium for Fossil Fuel Liquefaction Science (administered by the University of Kentucky). Dr. W. Windig and Mrs. M. Van are acknowledged for invaluable discussion in data analysis and manuscript preparation. We also acknowledge the superior cooperation of the staff of the Wilsonville Alabama pilot plant.

REFERENCES

1. Taghizadeh, K., Davis, B., Meuzelaar, H.L.C., 35th Annual Conference on Mass Spectrometry and Allied Topics., May (1987).
2. Leco Corp., CHN-600 Instrument Manual No. 200-340 (1983).
3. Unterzaucher, J., Analyst., 77, 584 (1952).
4. Leco Corp., SC-132 Manual 200-170 (1980).
5. Schultz, H., Mima, M.J., Prep. Pap., Am. Chem. Soc. Div. Fuel Chem., 23, (2)768, (1978).
6. Davis, B., Thomas, G., Sagues, A., Jewitt, C., Baumert, K., IMMR 80/053, April (1980).
7. Burke, F.P., Winschel, R.A., Pochapshky, T.C., U.S. DOE Contract DE-AC05-79ET-14503, Final Report, FE-14503-3., November (1983).
8. Levy, G.C., Nelson, G.L., Carbon-13 Nuclear Magnetic Resonance for Organic Chemists, John Wiley and Sons., New York (1972).
9. Windig, W., Meuzelaar, H.L.C., 34th Annual Conference on Mass Spectrometry and Allied Topics., 64, (1986).
10. Windig, W., Meuzelaar, H.L.C., Anal. Chem. 56, 2297, (1984).
11. Windig, W., Meuzelaar, H.L.C., Haws, B.A., Campbell, W.F., Asay, K.H., Anal. Appl. Pyrolysis 5, 183, (1983).
12. Halma, G., Van Dam, D., Haverkamp, J., Windig, W., Meuzelaar, H.L.C., J. Anal. Appl. Pyrolysis., 7, 167, (1984).
13. Wozniak, T.J., Hites, R.A., Anal. Chem. 57, 1320, (1985).
14. Winschel, R.A., Burke, F.P., Proceedings 8th Annual EPRI Contractors Conference on Coal Liquefaction, (1983).

TABLE I
AVERAGED NMR AND CONVENTIONAL CHARACTERIZATION DATA FOR HYDROTREATER FEED
AND HYDROTREATER PRODUCT SAMPLES

Conventional Parameters*	Hydrotreater Feed (%)	Hydrotreater Product (%)	NMR Parameters*	Hydrotreater Feed (%)	Hydrotreater Product (%)
C {1 2 3}	88.70±0.13 88.82±0.28 88.67±0.37	88.89±0.19 89.25±0.14 89.08±0.41	Condensed Aromatics {1 2 3}	18.01±1.16 12.00±0.76 26.18±3.59	12.01±1.06 7.85±0.53 19.89±4.80
H {1 2 3}	7.67±0.07 8.85±0.25 5.69±0.08	8.73±0.23 9.76±0.09 6.13±0.25	Noncondensed Aromatics {1 2 3}	8.26±1.21 9.95±1.33 10.09±1.93	6.00±0.57 4.87±0.33 7.34±1.98
N {1 2 3}	0.83±0.06 0.46±0.02 1.98±0.07	0.70±0.12 0.29±0.04 1.68±0.07	Cyclic Alpha {1 2 3}	17.33±0.76 13.08±1.64 18.77±1.67	17.73±0.65 14.70±1.72 19.76±0.82
S {1 2 3}	0.41±0.01 0.24±0.02 0.59±0.02	0.18±0.05 0.03±0.01 0.49±0.25	Alkyl Alpha {1 2 3}	9.89±0.71 10.50±0.60 10.95±0.63	10.03±0.29 9.27±0.49 11.03±0.54
O {1 2 3}	2.38±0.12 1.62±0.12 3.06±0.31	1.51±0.12 0.67±0.08 2.63±0.58	Cyclic beta {1 2 3}	13.73±2.48 16.41±0.75 13.52±0.71	20.19±0.35 20.35±1.28 16.42±1.35
Phenols	1.27±0.30	0.36±0.14	Alkyl beta {1 2 3}	20.61±0.95 22.54±0.70 12.86±1.02	21.22±0.66 24.31±0.77 13.58±1.56
Distillate	56.13±3.53	65.29±4.24	Gamma {1 2 3}	12.17±1.06 18.46±2.61 7.63±0.92	12.81±0.43 18.64±2.89 11.98±4.03
Nondistillate	43.87±3.53	34.71±4.24	Aliphatic Aromatic {2 2}	52.81±1.64 33.23±1.55	64.20±2.16 24.16±1.53
Oils	58.28±1.60	75.79±2.90	Aromatic {2}	13.97±1.49	11.64±1.47
Asphaltenes	30.02±1.44	20.42±2.28			
Benzene Insol.	11.70±1.53	3.79±1.10			

* (1) total sample, (2) distillable, and (3) nondistillable fraction.

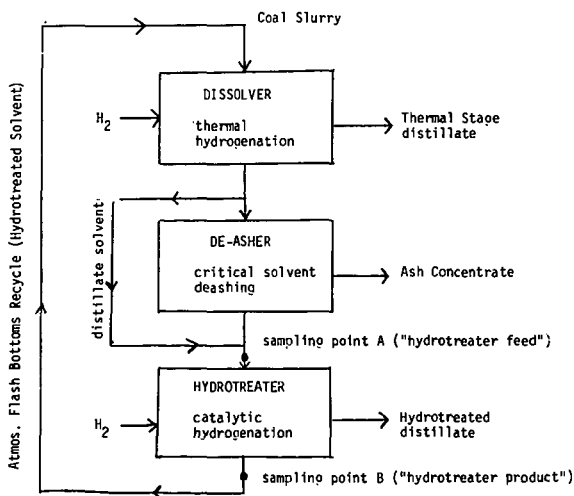


Figure 1. Wilsonville Integrated Two Stage Liquefaction (ITSL) process (simplified scheme).

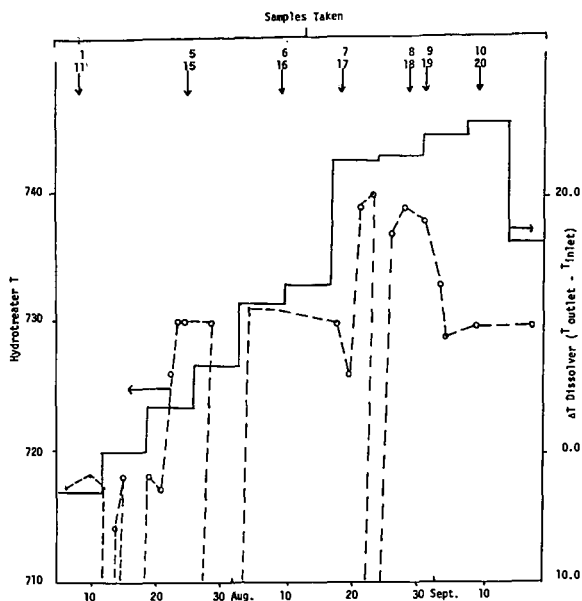


Figure 2. Temperature/-time profile of hydro-treater (—) as well as a seven day average of the difference (ΔT) between the outlet and inlet temperature of dissolver (---) and days on which samples were collected.

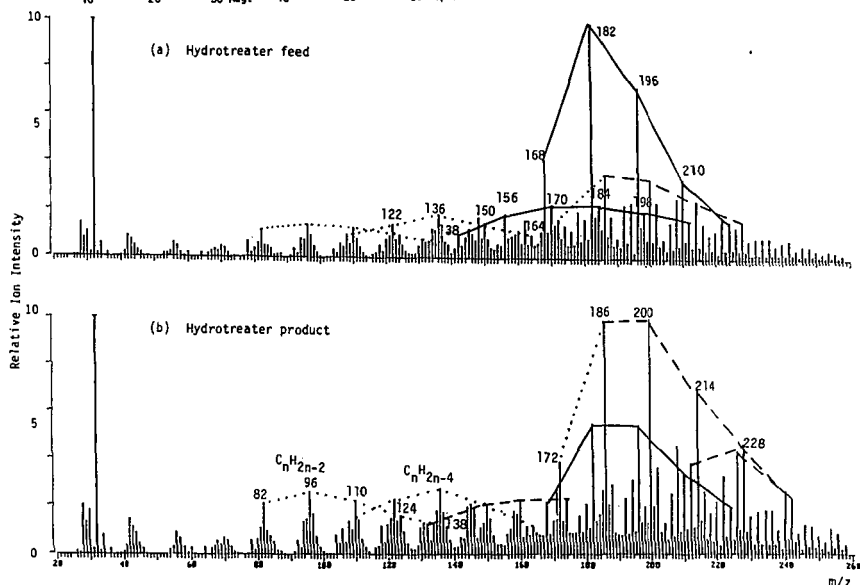


Figure 3. Averaged low voltage mass spectra of the hydrotreater feed (a) and hydrotreater product (flash bottoms) (b).

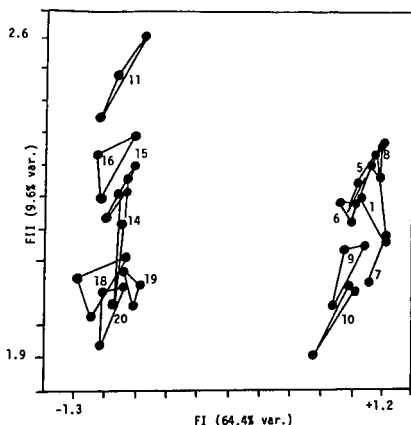


Figure 4. Factor score plot of low voltage MS data in the Factor I and Factor II subspace. Triplicate analyses of the same sample are connected by solid lines. For sample codes see Figure 2.

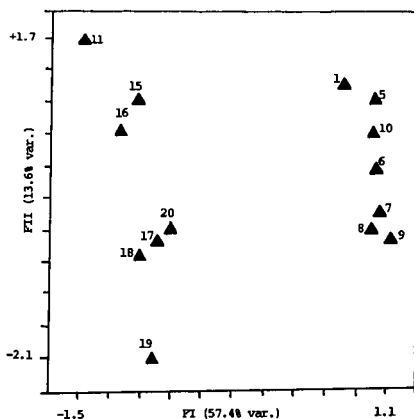


Figure 5. Factor score plot of NMR and conventional data in the Factor I and Factor II subspace, showing two cluster hydrotreater feed (1-10) and hydrotreater product (11-20). For sample codes see Figure 2.

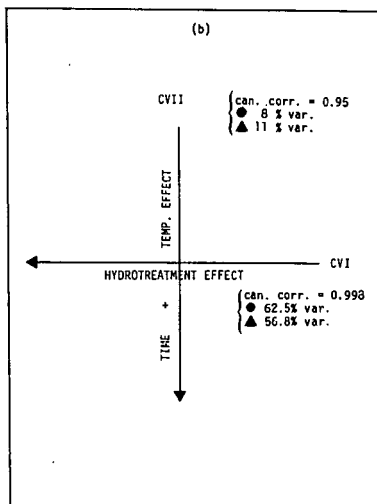
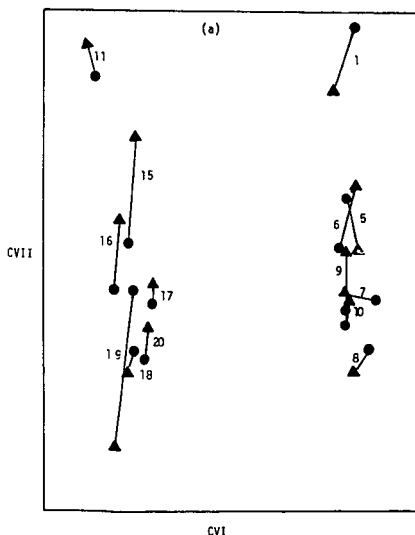


Figure 6. (a) Scores of low voltage MS (●) and scores of NMR and conventional data (▲) in the CVI and CVII subspace. Note the correlation between two data sets. (b) Interpretation of the major trends in the CVI-CVII subspace.

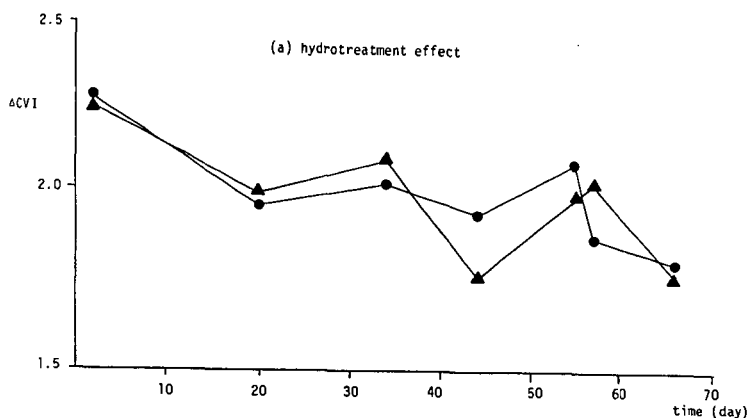


Figure 7. Absolute differences of CVI scores of hydrotreater feed and hydrotreater product for low voltage MS (●) and NMR and conventional data (▲).

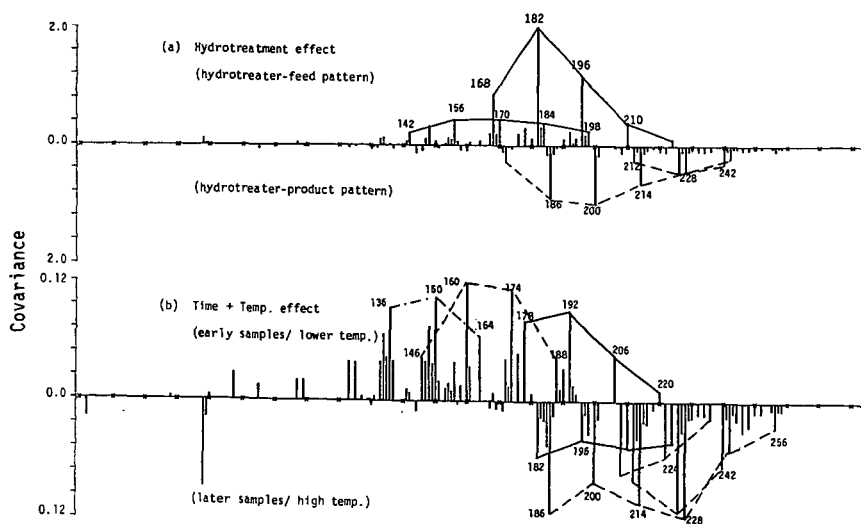
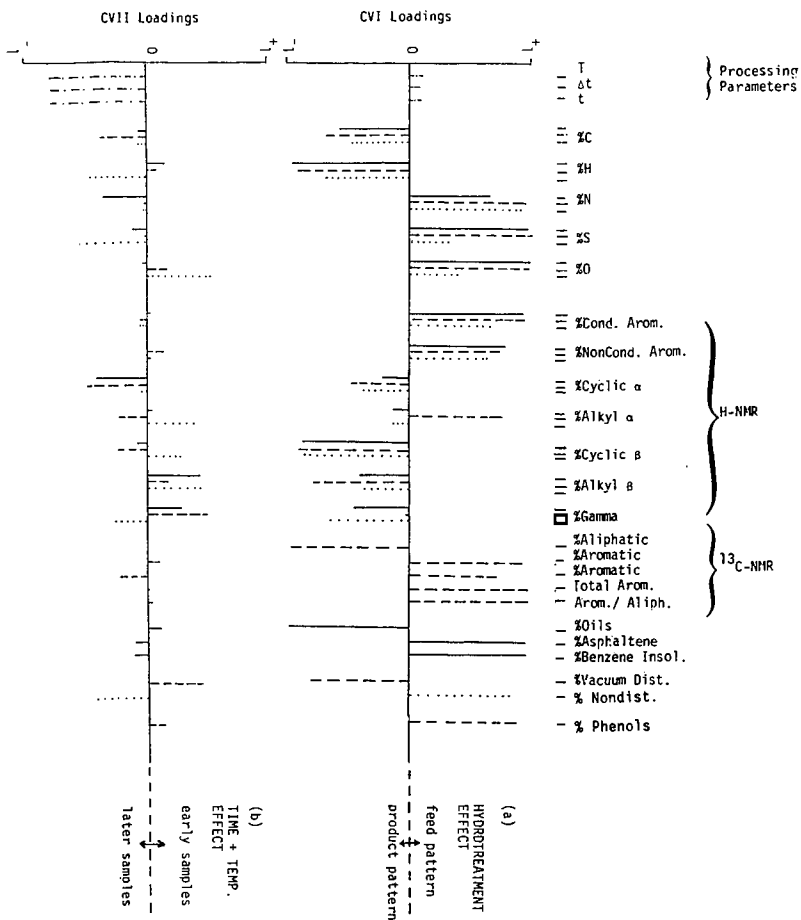


Figure 8. Mathematically extracted spectra of low voltage MS on CVI rotation (a) and CVII rotation (b).

Figure 9. Loading of NMR and conventional variables on CVI (a) and CVII (b). Total sample (-), distillable fraction (---) and nondistillable fraction (...).



CONVERSION OF TETRALIN TO NAPHTHALENE DURING COAL LIQUEFACTION:
A COAL RANK PHENOMENON?

B. Chawla, R. Keogh and B. H. Davis

Kentucky Energy Cabinet Laboratory
P. O. Box 13015
Lexington, KY 40512

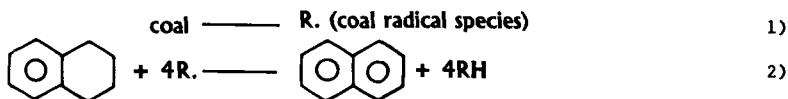
ABSTRACT

Since coal conversion, in the presence of tetralin (a donor solvent), is believed to be a coal rank phenomenon, it seemed worthwhile to determine the role of rank upon conversion of tetralin (T) to naphthalene (N) during coal liquefactions at 385°, 427° and 445°C. The THF soluble fractions, containing T and N, were analyzed using a high performance liquid chromatographic technique. The T/N ratios, for eight coal samples of different ranks, showed a direct relationship between the coal rank and the T/N ratio. The conversion of tetralin to naphthalene was lowest for the highest rank coal, and vice versa. The T/N ratio versus rank relationship was obtained for reaction times ranging from 5 to 65 minutes.

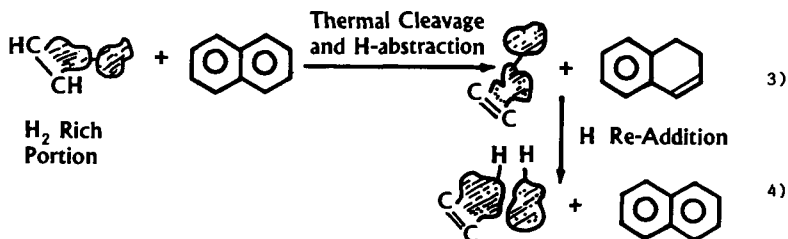
INTRODUCTION

Coal liquefaction processes have been studied in the presence of hydrogen donor as well as non-hydrogen donor solvents during the last five decades (e.g. 1-14). Two generally accepted pathways (5, 6, 14-17) for H-transfer from a donor solvent (tetralin) to coal during coal liquefactions are shown in equations 1) to 4).

Pathway I



Pathway II



Higher coal conversions in the presence of donor solvents have established that no matter which pathway dominates, the solvent hydrogen donor ability plays an important role in the process of coal liquefaction. However, only a small fraction of the research efforts, which are presently being made towards coal liquefaction processes, is being devoted for understanding the fate of H-donor solvent.

Tetralin (a donor solvent) involvement during coal liquefaction processes is indeed highly complex (3, 4, 16, 18) and produces various compounds such as naphthalene, 1-methylnaphthalene, 1-methylindane, indane, indene, butylbenzene, dimers and C₉ - C₁₁ hydrocarbons, etc. However, the major component of tetralin conversion is naphthalene. In order to determine the role of coal rank upon conversion of tetralin (T) to naphthalene (N), we report in this paper our results on T/N ratios for liquefaction of eight coals of different ranks at 385°, 427° and 445°C.

EXPERIMENTAL

The liquefaction experiments were conducted in a microautoclave reactor of 50 ml capacity. The microautoclave was charged with 5g of coal (-100 mesh, dried overnight under vacuum of about 25 inches of Hg at 80-90°C), 7.5g of tetralin and a steel ball (1/4" dia.) for mixing. The system was pressurized with 800 psi of H₂ at ambient temperature (ca. 2000 psi at 445°C) and immersed in a heated sand bath for the desired reaction time. Typically, it required less than two minutes to reach the desired reaction temperature. To ensure thorough mixing of ingredients, the shaker speed (vertical) was set at 400 cpm. At the end of the experiment, the reactor was inserted in a cold sand bath. Once the reactor had come back to ambient temperature (within two minutes), the unreacted H₂ and other gases were slowly released. The products were removed from the reactor using tetrahydrofuran (THF) and were extracted in Soxhlet equipment to obtain the coal conversion. The extraction was continued for about 24 hours or more until the liquid extract obtained was clear.

The THF soluble reactor products were analyzed by a high performance liquid chromatographic (HPLC) technique. The technique requires only the stirring of resulting reactor products overnight with excess of THF and then injecting the THF filtrate into the HPLC system. The ratio of peak areas (number of counts) of tetralin and naphthalene can be used to obtain the T/N ratio directly (without knowing solution concentration) from a linear calibration plot of Tarea/Narea versus T/N (see Figure 1). This technique was developed by optimizing the conditions for the analysis of the THF soluble reactor products:

Column: Supelcosil, LC-PAH (25cm x 4.6mm)
Mobile Phase: THF: H₂O, 40:60
Flow: 0.9 ml/min
Detector: UV, λ 254 (nm)

The performance of the HPLC system was checked against a standard mixture of uracil, acetophenone, benzene and toluene with CH₃OH:H₂O, 60:40 as a mobile phase with a typical flow rate of 1 ml/min.

The precision and reproducibility of the data were established by making repeated measurements for completely independent experiments performed on different days. The precision of the T/N data was found to be better than 1%. The accuracy of our results was verified by comparing the T/N ratios obtained by gc and HPLC. The maximum uncertainty in the T/N ratios was determined to be less than 5%.

The HPLC grade THF and water and the commercially available tetralin were used as supplied.

The chemical analyses of the eight coals used in this work are presented in Table 1.

RESULTS AND DISCUSSION

Effect of Coal Rank and Temperature on T/N Ratio

Coal liquefaction runs for eight coal samples were made at three temperatures, 385°, 427° and 445°C, to determine the extent of conversion of tetralin to naphthalene. The tetralin/naphthalene ratios obtained for the THF soluble reactor products are presented in Table 2. The overall variation in T/N values from 1.80 to 18.7 is very significant for the range of coal ranks covered under this study. The following observations result from the data in Tables 1 and 2:

- (a) T/N ratio decreases with an increase in reaction temperature for all the coals studied.
- (b) T/N ratio decreases with an increase in oxygen content of the coal. The decrease of the T/N ratio with the increase in oxygen content is much more systematic at the 427° and 445°C thermal severities, the data for 385°C are somewhat scattered.
- (c) T/N ratio decreases with a decrease in carbon content of the coal and again the decrease in T/N ratio is more systematic at 427° and 445°C.
- (d) The percentage coal conversion to THF soluble products (data not given in Table 2) increases with an increase in temperature - consistent with the previous observations (5, 17). Therefore, as the T/N ratio decreases, the conversion of THF soluble product increases. This relationship holds true for a particular coal at the three thermal severities: 385°, 427° and 445°C. However, this relationship does show considerable scatter when one tries to relate the T/N ratios with the conversion data for a series of coals at the higher reactor temperatures such as 445°C. This is most likely due to the secondary reactions taking place, i.e., asphaltenes and/or preasphaltenes to produce oils and gases.

As the coal rank decreases (the carbon content decreases and oxygen content increases) there will be an increase in hydrogen demand during coal liquefaction process. The higher the hydrogen consumption during the reaction, the higher is the conversion of tetralin to naphthalene. Hence the result is a lower T/N ratio. This is consistent with the observations discussed previously under (b) and (c). Therefore, the lower the coal rank, the lower is the T/N value (or higher H_2 demand).

We have made several attempts to correlate T/N ratios with various other properties of coals. However, there seem to be no other reportable relationships with the limited data base available at present.

Effect of Liquefaction Duration on T/N Ratio

In order to determine the effect of liquefaction residence time (kinetic versus equilibrium conversions) on the T/N ratio, experiments were performed at 445°C for reaction times ranging from 5 to 65 minutes. The T/N ratios obtained using two coals of different ranks (a Western Ky. #9 and a Wyodak) are presented in Figure 2. Figure 2 also displays the T/N results obtained for blank experiments performed on tetralin + H_2 in the presence of a catalyst (Ni/Mo oxide).

As shown in Figure 2, the T/N value decreases sharply with the increase in reaction time until it reaches some pseudoequilibrium value for both the coals and the blank experiments. However, the T/N values obtained for the catalytic tetralin experiments achieve a pseudoequilibrium value faster than those of coals. All reactor conditions were constant in these experiments except different coal samples and a Ni/Mo oxide catalyst for the blank runs were used. Since the pseudoequilibrium values are different for the two coals the pseudoequilibrium T/N value also appears to be coal rank dependent. The relatively low and different pseudoequilibrium T/N values for the two coals (1.3 and 1.9) as compared to that of the catalyzed (Ni/Mo) tetralin conversion reaction (4.0) clearly suggest that the conversion of tetralin to naphthalene is mainly due to the extent of the hydrogen demand during liquefaction rather than some catalytic reactions from the mineral matter. This is further supported by the fact that there was no significant conversion of tetralin to naphthalene when tetralin was heated with or without low temperature ash in presence of H_2 at 385°, 427° and 445°C.

The parallel behavior of T/N ratios of two coals of different ranks over the entire range of reaction time suggests that the T/N ratios (Figure 2) follow a parallel course in both the kinetic (ca. first 35 minutes) and the equilibrium processes (> 35 minutes) and the major contribution to T/N ratio is probably through kinetically controlled processes. This phenomenon is partially supported by the fact that the conversion for most of the coals reaches its maximum value within 5 to 10 minutes (5, 17, 19).

In order to compare and understand the contributions from kinetically and thermodynamically controlled processes to T/N ratios, liquefaction experiments, using a 45 minute residence time and a 445°C reactor temperature, were performed using the eight coals. The T/N ratios obtained using the longer residence time and the 15 minute residence time are compared in Figure 3. As can be seen, a linear relationship with a slope of greater than unity (1.23) clearly suggest that tetralin is also involved in the

thermodynamically controlled process and the extent of tetralin conversion is controlled by the coal rank. Since coal conversion to THF solubles are somewhat similar (ca. 90%) for 15 minute and 45 minute liquefaction runs, the question arises: what does tetralin do during thermodynamically controlled process? One possible explanation is that during the thermodynamically controlled process, the coal rank dependent conversion of tetralin to naphthalene is due to the hydrogen demand of the secondary reactions of asphaltenes and preasphaltenes to produce the lower molecular weight components - oils and gases. On the other hand, the coal rank dependent conversion of tetralin to naphthalene during kinetically controlled process of coal dissolution is possibly due to the hydrogen demand of the production of asphaltenes and preasphaltenes from the coals. This needs to be clarified further by analyzing the liquefaction products obtained using the different reaction times and is under investigation in our laboratory.

ACKNOWLEDGEMENT

This work was supported by the Commonwealth of Kentucky, Kentucky Energy Cabinet and DOE Contract No. DEFC22-85PC80009 as part of the Consortium for Fossil Fuel Liquefaction Science (administered by the University of Kentucky).

REFERENCES

1. Pott, A.; Broche, H.; Schmitz, H.; Scheer, W., Gluckauf 1933, 69, 903.
2. Orchin, M.; Storch, H. H., Ind. Eng. Chem. 1948, 40, 1259.
3. Curran, G. P.; Struck, R. T.; Gorin, E., Ind. Eng. Chem. Process Des. Dev. 1967, 6, 166.
4. Wiser, W. H., Fuel 1968, 47, 475.
5. Neavel, R. C., Fuel 1976, 55, 237 and references cited therein.
6. Tsai, M. C.; Weller, S. W., Fuel Process Technol. 1979, 2, 313.
7. "Solvent Activity Studies" DOE/PC/50041-18, DE83, 015870, Catalytic Inc., Wilsonville, Alabama.
8. "Coal Liquefaction - The Chemistry & Technology of Thermal Processes" by D. D. Whitehurst et al., Academic Press, 1980.
9. Derbyshire, F. J.; Whitehurst, D. D., EPRI Contractor's Meeting, May 1980, Palo Alto, California.
10. Derbyshire, F. J.; Odoerfer, G. A.; Rudnick, L.R.; Varghese, P.; Whitehurst, D. D., EPRI Report, AP-2117, Vol. 1, Project 1655-1, 1981.
11. Ohe, J.; Itoh, H.; Makaba, M.; Ouchi, K., Fuel 1985, 64, 902 and 1108.
12. Skowronski, R. P.; Ratto, J. J.; Goldberg, I. B.; Heredy, A., Fuel 1984, 63, 440.

13. Besson, M.; Bacaud, R.; Charcosset, H.; Cebolla-Burillo, V.; Oberson, M., *Fuel Process Technol.* 1986, 12, 91.
14. Storch, H. H., "Chemistry of Coal Utilization", Ed.: H. H. Lowry, Vol. II, John Wiley and Sons, 1945.
15. Heredy, L. A.; Fugasi, P., "Phenanthrene Extractions of Bituminous Coal", *Coal Science Advances in Chemistry Series*, No. 55, 1966, 448.
16. Whitehurst, D. D.; Farcasiu, M.; Mitchell, T. O., *The Nature and Origin of Asphaltenes in Processed Coals*, EPRI-AF-252, 1st Annual Report, Palo Alto, CA 1977.
17. Pina, B. B., "Hydroliquefaction Performance of Two Kentucky Coals in Solvents of Various Hydrogen-Donor Strengths", M.S. Thesis, 1984, University of Louisville, Louisville, Kentucky and references cited therein.
18. (a) Poutsma, M. L.; Youngblood, E. L.; Ostwald, G. E.; Cochran, H. D., *Fuel* 1982, 61, 314. (b) Shah, Y. T.; Cronaur, D. C., *Catal. Rev. - Sci. Eng.* 1979, 20, 209 and references therein. (c) Vernon, L. W., *Fuel* 1980, 59, 102. (d) Collins, C. J.; Raaen, V. F.; Benjamin, B. M; Maupin, P. H.; Roark, W. H., *J. Am. Chem. Soc.* 1979, 101, 5009. (e) Franz, J. A.; Camaioni, D. M., *J. Org. Chem.* 1980, 45, 5247. (f) Berman, M. R.; Comita, P.B.; Moore, C. B.; Bergman, R. G., *J. Am. Chem. Soc.* 1980, 102, 5692 and references therein.
19. Our unpublished results.

Table 1. Coal Analysis.

	W. Ky. #9 71154	Breckinridge 71160	W. Ky. #9 71072	W. Ky. #11 71064
1. Ash (As-Received)	30.03	6.36	9.04	9.56
2. Volatile Matter, daf	47.83	74.28	42.90	47.47
3. Fixed Carbon, daf	52.17	25.72	57.10	52.53
4. Sulfate S, daf	0.00	0.01	0.14	0.06
5. Pyritic S, daf	1.47	1.23	0.53	1.06
6. Organic Sulfur, daf	2.27	0.55	1.91	3.11
7. Total Sulfur, daf	3.74	1.81	2.57	4.23
8. Carbon, daf	84.99	80.66	79.19	78.80
9. Hydrogen, daf	6.16	8.51	5.44	5.85
10. Nitrogen, daf	1.98	2.13	2.00	1.70
11. Oxygen, daf	3.13	6.90	10.80	9.42

	W. Ky. #11 71081	G. Seam-Co. PSOC866	Wyodak-Wy. 91168	Fort Union Bed-Mt. PSOC833
1. Ash (As-Received)	4.43	17.80	6.64	10.22
2. Volatile Matter, daf	43.23	36.96	52.92	46.86
3. Fixed Carbon, daf	56.77	63.04	47.08	53.14
4. Sulfate S, daf	0.17	0.04	0.05	0.07
5. Pyritic S, daf	0.64	0.06	0.17	0.12
6. Organic Sulfur, daf	2.21	0.52	0.78	0.46
7. Total Sulfur, daf	3.01	0.62	1.00	0.64
8. Carbon, daf	78.28	75.20	71.02	68.64
9. Hydrogen, daf	5.52	5.34	5.42	4.72
10. Nitrogen, daf	1.70	1.18	1.37	1.26
11. Oxygen, daf	11.49	17.66	21.29	24.74

Oxygen by difference.

Table 2. *T/N Ratios for 15-Minute Duration Liquefactions at Three Temperatures and THF Soluble Conversions at 445°C.*

Coal Sample	Conversion (%)		T/N Ratio		
	445°C 15 min.	445°C 45 min.	445°C	427°C	385°C
71154 (Ky. #9)	—	94.6	4.03 ± 0.21	6.63 ± 0.62	17.40 ± 1.0
Breckinridge	—	90.6	3.51 ± 0.27	5.96 ± 0.18	18.7
71072 (Ky. #9)	—	87.6	2.78 ± 0.12	4.30 ± 0.15	10.3 ± 0.5
71064 (Ky. #11)	—	95.1	2.62 ± 0.06	3.70 ± 0.11	9.14 ± 0.05
71081 (Ky. #11)	93.6	92.7	2.37 ± 0.25	3.99 ± 0.13	11.13 ± 0.22
PSOC 866	77.2	80.2	1.86 ± 0.06	—	—
91648 (Wyodak)	89.5	90.0	2.07 ± 0.06	2.60 ± 0.04	—
PSOC 833	—	84.0	1.80 ± 0.05	2.86 ± 0.05	6.30 ± 0.10

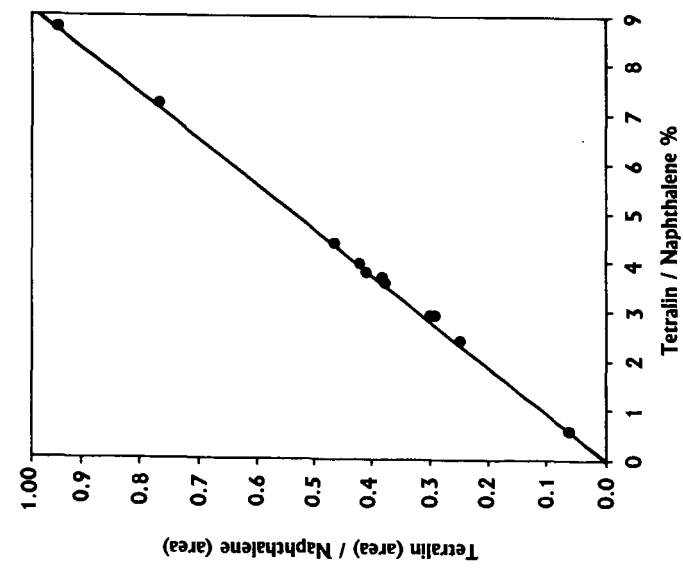


Figure 1. Ratios of Peak areas versus T/N (wt. %) Ratios.

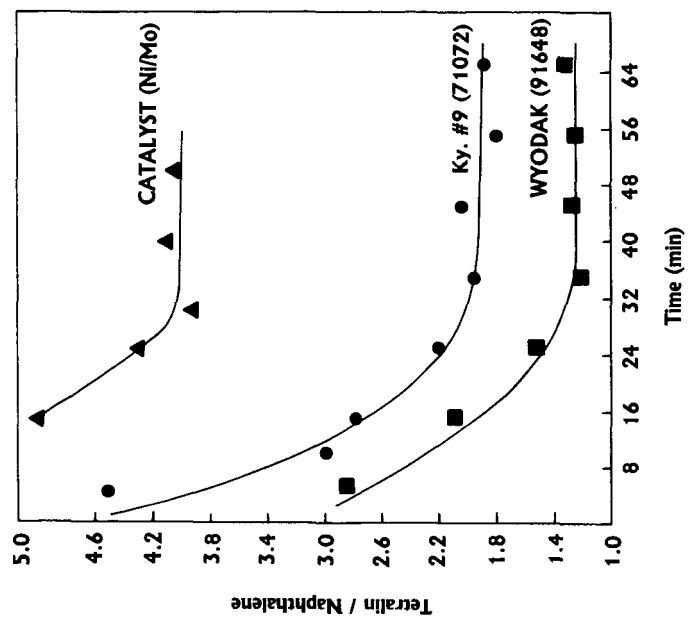


Figure 2. T/N Ratios at 445°C.

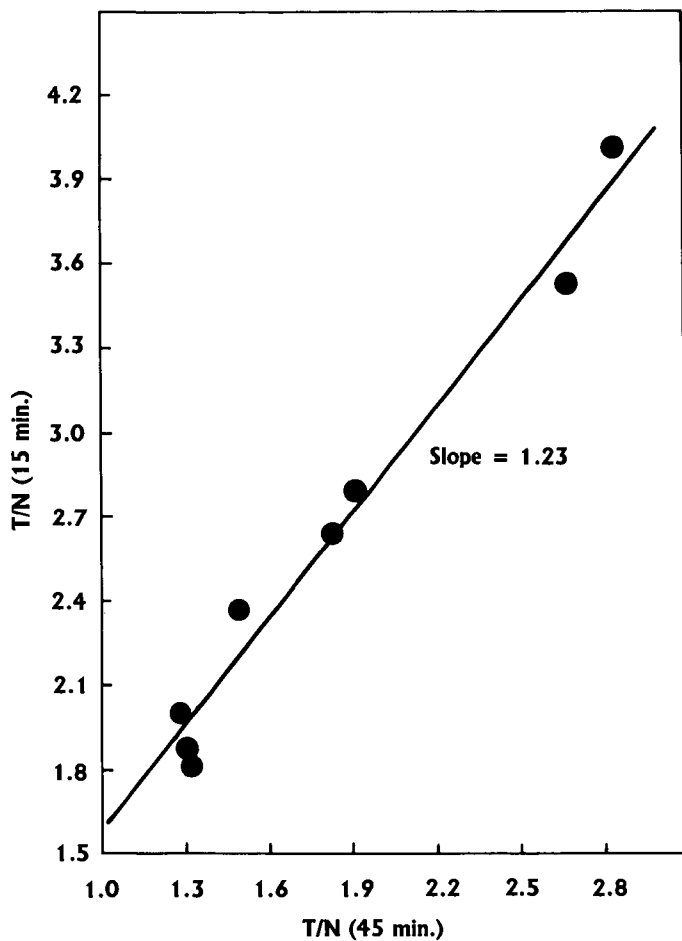


Figure 3. Comparison Between the T/N Ratios of 15 and 45 Minutes Residence Time Runs at 445°C .

THE ORGANIC/MINERAL INTERACTION IN COAL LIQUEFACTION BOTTOMS

W.A. Leet, F.S.-C. Lee, R. Gandy, and D.C. Cronauer

Amoco Oil Corporation
P.O. Box 400
Naperville, IL 60566

ABSTRACT

Characterization of the organic/mineral matter interactions is central to the problem of solid/liquid separation in the liquefaction of coal. Samples of the vacuum tower bottoms from the liquefaction of Illinois No. 6 coal in the Wilsonville pilot plant have been studied. The techniques include various analyses such as elemental, solvent extraction, STEM, FTIR, XPS, XRD, and XRF. Surface active oxygenates associated with organic/mineral matter interaction appear to consist of both phenolics and carboxylates. The observed characteristics of the organic/mineral interactions were affected by the recycle of mineral matter and unconverted coal as part of the liquefaction feed solvent.

INTRODUCTION

The separation of unconverted coal and mineral matter from heavy coal-derived liquids is difficult. Work was undertaken to determine if an interaction between these components could be demonstrated which could prove useful in the design of efficient mineral removal processes. Specific reference is made to the use of critical solvent deashing (CSD) such as that of the ROSE-SR process of Kerr-McGee Corporation. The polar functionality of clays, carbonates, and other minerals would likely interact with heterofunctional groups in coal asphaltenes and preasphaltenes. Therefore, typical coal-derived resids and unconverted coal solids were characterized, focusing on the loading of organic oxygenates onto mineral matter.

Coal asphaltenes have been shown to have high levels of heterofunctionality(1), and the oxygenate groups are primarily phenolic(2) with low to immeasurable levels of carboxylic groups. In fact, Illinois No. 6 coal, which was used to generate the products tested in this study, was shown to contain about one-tenth(2) or less(3) of its oxygen as carboxylic groups. In addition, it has been shown(4) that coal loses carboxylic groups on heating to elevated temperatures. Therefore, since this functionality was observed in the heavy fractions and CSD operation greatly improved with the recycle of unconverted coal, we extended this study to include the characterization of recycled solids which may have served as catalytic sites for liquid upgrading and/or coking. Reference is made to the work of Wakeley, et al.(5) with respect to the nature of reactor solids accumulating during liquefaction.

EXPERIMENTAL

Samples were obtained from the Advanced Coal Liquefaction R&D Facility at Wilsonville, AL, which has been described by Lamb, et al(6). The Wilsonville pilot plant was operating in a two-stage mode with direct coupling of the thermal and catalytic (hydrotreater) reactors as shown in the schematic, Figure 1. After flashing and vapor recovery, the vacuum tower bottoms (VTB) cut was fed to a critical solvent deashing (CSD) unit to reject an ash concentrate and recover an ash-free resid. The products of two runs were studied. In run 250D, the liquefac-

tion feed solvent consisted of recycled flash distillates plus CSD-derived resid. In run 250H, a portion of the VTB, including unconverted coal and mineral matter, was added to the feed solvent. Both runs were made with Illinois No. 6 coal at essentially the same reaction conditions, and CSD operation was shown (7) to be much smoother in the latter run.

Characterization data for samples of VTB of these two runs are summarized in Table I. GPC analysis of the organic Soxhlet fractions produces identical molecular weight profiles for the two samples. The data document the higher concentration of mineral matter and unconverted coal in run 250H product as a result of recycle. The shift in the Soxhlet characterization data, specifically the decrease in the oils (pentane solubles) content, highlights a significant shift in character as a result of process recycle. Apparently, recycle leads to increased solubilization and reaction of the heavy fractions in the liquefaction reactors resulting in a more refractory resid.

The VTB cuts resids were Soxhlet extracted with tetrahydrofuran (THF) to separate the soluble organic matter from the solids. NMR analysis of the THF extracts is provided in Table II. There are large differences in the aliphatic carbon and ring size (bridgehead carbon) between the two samples. Run 250H VTB is more highly dealkylated ($C_{a-s} = 12.2$ vs. 18.3%) and condensed ($C_{a-i} = 27.2$ vs. 18.6%). This is consistent with the lower level of oils found in the VTB upon recycle. FTIR data confirm the observation. FTIR analysis also points to a nearly five-fold increase in the phenolic oxygen content of run 250D product over that of 250H. This difference is largely due to THF extractables.

The physical makeup of the THF insolubles fraction of both runs was examined by Dr. Alan Davis of Pennsylvania State University using petrographic techniques. The results indicate that the organic portion of the fractions were primarily composed of vitropast (20 vol %), unreacted "inertinite" (9-12 vol %), and unreacted vitrinite (2-8 vol %). The 250D sample contained larger amounts of unreacted inertinite than the 250H sample. The 250H sample also contained masses of larger vitropast spheres (secondary vitropast) which were not seen in the 250D sample. No mesophase structures were observed and only very rare particles of coke were noted in the residues. Both samples exhibited large amounts of clays (50-55 vol %) and iron sulfides (6-13 vol %). While the clay concentrations were similar for both fractions, the concentration of iron sulfides in the 250H VTB were twice that in the 250D sample, reflecting the concentration of mineral matter by process recycle. Trace (1-4 vol %) carbonates were also identified. However, the carbonates, present also in the feed coal, were highly crystalline and exhibited none of the structure of the reactor-formed carbonates which are generated during the processing of some carboxylate-rich low-rank coals.

The mineral matter concentrated in the THF insolubles was analyzed by XRF and XRD. Analysis by XRF shows that the mineral matter of the two samples to be similar in composition (Table III), with large amounts of silicon, alumina, and iron present. XRD analysis shows the latter three components to be in the form of α -quartz, iron sulfide minerals (predominantly pyrrhotite), and aluminosilicates (principally kaolinite). Both samples exhibit traces of carbonates as noted earlier.

Ground particles of VTB before and after THF extraction were characterized by STEM and XPS. STEM analysis points to the agglomeration of iron sulfide and calcium mineral particles upon THF extraction. XPS data for mineral matter for both resids

before and after THF extraction are summarized in Table IV. The data indicate high levels of physical adsorption of organic matter on the silicate and aluminosilicate mineral surfaces in that the organic coating is removed by THF extraction. However, the iron sulfide surface exhibits significant irreversible adsorption or coking on the surface, because organics are not removed by THF extraction. A similar situation exists for calcium carbonate surfaces, but to a lesser extent than that of iron sulfide.

Elemental analysis of the organic matter in the THF insolubles fractions of the VTB cuts is given in Table V. The THF insolubles fractions of both VTB cuts are similar with significant concentrations of heteroatoms in the THF insolubles. Much of the organic oxygen shows up as strong phenolic oxygen absorption in the OH/NH stretch region of the FTIR spectrum (Figure 2). Comparison of ratios of normalized integrals and normalized intensities of the second derivatives by deconvolution shows that like amounts and types of phenolics are concentrated in the THF insolubles fractions of the two VTB cuts. The FTIR spectra also exhibit small but marked residual carboxylic acid absorption at around 1700 wavenumbers and a carboxylate band around 1530 (Figure 3). In comparison to the very weak carboxylic signal in the whole VTB, the data indicate that the carboxylate functional groups are preferentially attached to the THF insolubles portion of the resid. Acidification of the THF insolubles with 6N HCl followed by extraction with CHCl₃ leads to a 44% reduction in the intensity of the carboxylic acid band in the insolubles, so there is interaction with the minerals that are removed by acid treatment.

CONCLUSIONS

The separation of unconverted coal and mineral matter at Wilsonville was shown to be better when a portion of these solids were recycled with the feed solvent to the liquefaction reactor. Our analysis of the VTB feed to the separation unit indicates that such recycle leads to increased solubilization of the heavy fractions and a more refractory (condensed) resid. We also observed that some carboxylic acid functionality is retained in the heavy coal-derived fractions after coal liquefaction. This appears to be due to an interaction of these groups with the mineral matter. It has also been observed that much of the carbonaceous deposits formed on the silica and aluminosilicate clays can be removed by extraction with a polar solvent, but the organic matter deposited on the iron sulfides and carbonates are more coke-like and not readily removed.

ACKNOWLEDGEMENT

The aid of Dr. A. Davis of Pennsylvania State University in the petrographic analysis of the samples is gratefully acknowledged. The analytical support of T. F. Fleisch, G. W. Fajac, J. B. Hall, and R. W. Tumbula and the suggestions of B. A. Fleming are also acknowledged. Personnel at Wilsonville were also instrumental in handling the appropriate samples.

REFERENCES

1. Whitehurst, D. D., Farcasiu, M., Mitchell, T. O., and Dickert, J. J., "The Nature and Origin of Asphaltenes in Processed Coals," EPRI AF-480, Project 410-1 Annual Report, July, 1977.
2. Ruberto, R. G., and Cronauer, D. C., in "Organic Chemistry of Coal," J. W. Larson, ed., Am. Chem. Soc. Symp. Ser., 71, 50, 1978.
3. Dutta, P. K., and Holland, R. J., Fuel, 62, 732, 1983.
4. Mragikova, J., Sindler, S., Veverka, L., and Macak, J., Fuel, 65, 342, 1986.
5. Wakeley, L. D., Davis, A., Jenkins, R. G., Mitchell, G. D., and Walker, P. L., Fuel, 58, 379, 1979.
6. Lamb, C. W., Nalithan, R. V., and Johnson, T. W., "Process Development Studies of Two-Stage Liquefaction at Wilsonville," Am. Chem. Soc. Div. Fuel Chem. Preprints, 31(4), 240, 1986.
7. Nalithan, R. V., Lee, J. M., and Johnson, T. W., "Status of Coal Liquefaction at Wilsonville," DOE Contractor's Review Conference on Direct Coal Liquefaction, Monroeville, PA, October. 20-22, 1986.

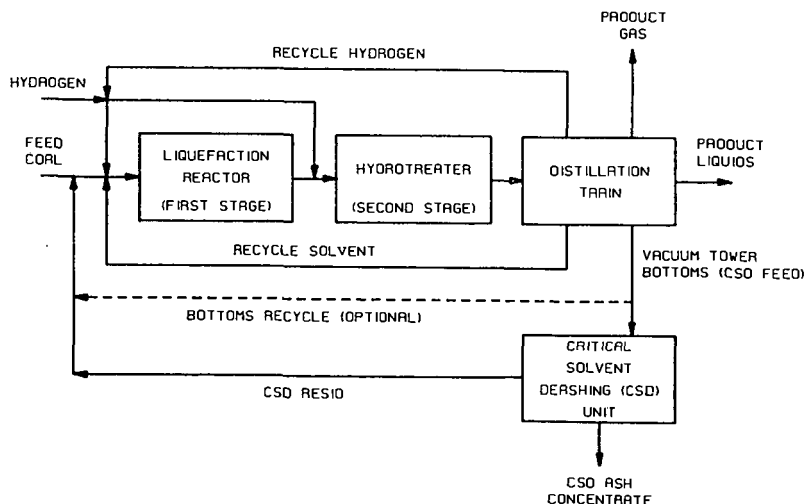


Figure 1. Wilsonville flowsheet.

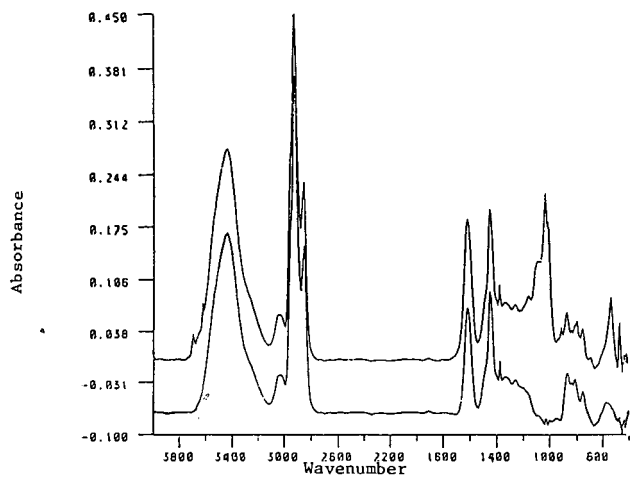


Figure 2 FTIR Spectra of Run 250D VTB and the HCl/CHCl_3 Insolubles from the VTB/THF Insolubles

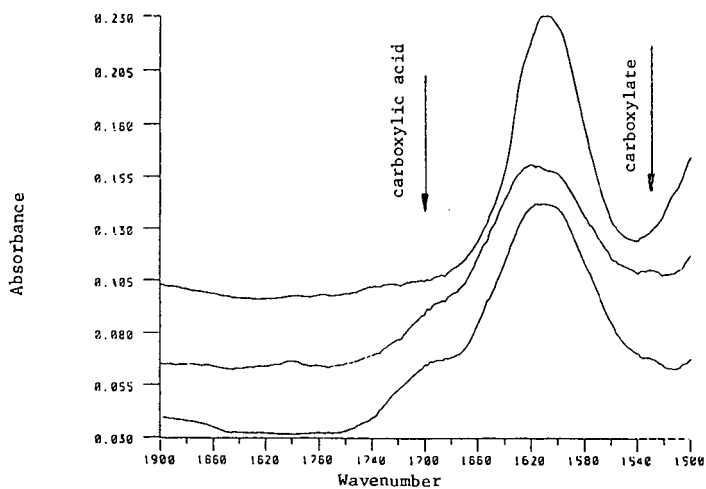


Figure 3 FTIR Spectra of Run 250H VTB (A), its THF Insolubles (B), and its HCl/CHCl_3 Insolubles

TABLE I

CHARACTERIZATION OF WILSONVILLE VACUUM TOWER BOTTOMS STREAMS

	<u>Run 250D</u>	<u>Run 250H</u>
<u>Proximate Analysis (wt%)</u>		
Moisture	0.09	0.10
Volatiles	67.8	58.1
Fixed Carbon (by diff.)	22.3	24.9
Ash	9.8	16.9
<u>Elemental Analysis</u> ¹ (wt%)		
Carbon	81.2	74.2
Hydrogen	6.29	5.43
Nitrogen	1.26	1.24
Sulfur	0.98	1.58
Oxygen	2.09	3.66
Atomic H/C	0.93	0.88
<u>Soxhlet Extraction</u> ² (wt%)		
Oils	46.4	29.3
Asphaltenes	24.0	21.4
Preasphaltenes	8.8	13.1
Coke & Unconverted Coal & Mineral Matter	20.8	36.2

¹ Uncorrected for mineral matter.

² Sequential extraction with n-pentane, toluene, and tetrahydrofuran.

TABLE II

NMR ANALYSIS OF THF EXTRACTS¹

	<u>Run 250D</u>	<u>Run 250H</u>
Ha, H on aromatic C	24.1	31.1
H _α , H on a C α to ring	35.4	25.6
Hsat, H on a C β or further to ring (=CH ₂ -)	31.3	35.4
Hme, H on CH ₃ γ or further to ring	9.2	7.8
Ca, aromatic ¹³ C	60.6	67.3
Cat. aromatic C bearing a H	23.7	28.0
Ca-s, aromatic C bearing an alkyl C	18.3	12.2
Ca-i, aromatic C at bridgehead position	18.6	27.2
Average number of rings ²	6	9

¹ Analyses based on combined ¹H and ¹³C-NMR. Data is expressed as % of total C or H.

² Average number of aromatic rings was calculated using a number average MW of 740 (VPO).

TABLE III

METAL COMPOSITIONS OF THF INSOLUBLES BY XRF

	<u>Run 250D</u>	<u>Run 250H</u>
Al	6.3	6.5
Na	<0.1	<0.1
Mg	0.18	0.22
Si	14.3	14.3
S	1.24	1.26
K	0.97	1.07
Ca	3.2	2.0
Ti	0.25	0.31
Fe	7.4	7.8
Ba	0.03	0.03
Mn	0.04	0.02
Total Metals	<u>34.0</u>	<u>33.5</u>
Oxide Ash	63.8	62.8

TABLE IV

ATOMIC RATIOS ON PARTICLE SURFACES AT RESIDS CALCULATED FROM XPS DATA¹

<u>Atomic Ratio</u>	<u>Run 250D</u>		<u>Run 250H</u>	
	<u>Whole Resid</u>	<u>THF Insol</u>	<u>Whole Resid</u>	<u>THF Insol</u>
Si/100C	1.0	11	0.8	10
Al/100C	0.0	7.3	0.6	7.1
Fe/100C	0.0	0.5	0.0	0.5
Ca/100C	0.0	1.0	0.0	1.5

¹ Adjusted to THF insolubles content basis.

TABLE V

ELEMENTAL ANALYSIS OF THF INSOLUBLES¹

	<u>Run 250D</u>	<u>Run 250H</u>
Carbon	29.5	29.8
Hydrogen	2.0	1.8
Nitrogen	0.5	0.8
Sulfur	4.4	4.3
Oxygen	6.5	5.9
Atomic H/C	0.83	0.73

¹ Uncorrected for mineral matter.

Catalyzed Reactions of Alkylaromatic Hydrocarbons Dissolved in Supercritical Fluids

F. C. Knopf, T.-H. Pang, K. M. Dooley

Dept. of Chemical Engineering, Louisiana State University
Baton Rouge, LA 70803

INTRODUCTION

Partial oxidations of alkylaromatic compounds occur at below 600K through catalytic mechanisms that are partly free radical in nature. These side chain oxidations and hydroxylations are usually catalyzed homogeneously by transition metal complexes or mixtures of metal salts with redox capabilities. Compounds of Co, Fe, and Mn are examples; the catalytic mechanisms exhibit certain common features (1-6). These are: (i) The ions have stable oxidation states separated by +1, because chain initiation and other reaction steps involve one-electron transfers; (ii) Once a reaction sequence (chain) is initiated, thermal free-radical steps occur in parallel with metal-catalyzed steps.

Alkylaromatics require less severe oxidizing conditions than do alkanes because of their smaller (by ~ 1 eV) ionization potentials, and partially oxidized side chains deactivate the ring for further reactions by this mechanism. Peroxides and hydroperoxides are the primary products of these oxidations, but these decompose to more stable products at temperatures above about 370K. As an example, consider the oxidation of toluene to benzaldehyde/benzoic acid. Four proposed reaction networks are shown in Figure 1. The initiation step involves electron transfer to Co^{3+} , suggesting that the trivalent ion is necessary for catalysis. However, the divalent ion reacts in several benzoperoxy decomposition steps, and in practice only small amounts of Co^{3+} are necessary.

An alternative to these liquid-phase processes is to use a supercritical fluid (SCF) phase to contact solid analogs of the homogeneous catalysts. Considering the above example of toluene oxidation, the use of an SCF phase would result in a homogeneous mixture and the removal of solubility limitations on O_2 . SCF mixtures have better mass transfer characteristics than typical liquids, and rapid reaction quenching of highly exothermic oxidations is possible by a pressure letdown from the SC region. A staged pressure letdown engenders another benefit, that of fractionation of reactants and products, eliminating the need for more complex downstream separations. Therefore it appears possible to exploit the capabilities of a SC mixture to provide a reaction medium for an entire class of what would normally be liquid phase oxidations. We are currently examining such catalytic oxidations in SCF-CO_2 for upgrading model coal liquid compounds that result from SCF extraction or flash hydropyrolysis processes. There are indications that alkylaromatic side-chain partial oxidation, which we have already demonstrated at SC conditions (7), will enhance the desired cracking reactions. For example, hydroxy groups ortho or para to methylene bridges facilitate bridge-bond rupture by allowing formation of a lower energy keto-enol tautomer intermediate; the half-life of the cleavage is reduced by over an order of magnitude (8). The presence of water causes cleavage of ether linkages to alcohols, which has

been observed for guaiacol pyrolysis at SC conditions (9). An example of these and similar reactions as applied to actual coal liquids is the autoxidation followed by anaerobic thermolysis of SRC in quinoline (10). The yield to combustion products at 388-453K was less than 10%.

RESULTS AND DISCUSSION

Preparing SCF-Aromatic Hydrocarbon Mixtures

Figure 2 gives the P-T diagram for a mixture of toluene and carbon dioxide as constructed from experimental data (11) and the Peng-Robinson equation of state (12), with the critical locus for a binary mixture computed by the algorithm of Heideman and Khalil (13). The TP-CP curves (1 = carbon dioxide and 2 = toluene) represent the vapor P curves for the pure liquids, from their triple points to their critical points. At point O the three-phase line ends (the liquid phases become identical) and the critical locus extends to CP₂ of pure toluene. Point a is in the SCF (F) region, point b is on the critical locus, and point c represents typical operating conditions (473K, 100 atm) for the initial reaction studies. The P-X diagram at 473K is given in Figure 3. The SCF phase on the left of the diagram contains at least 20 mol% toluene. The feed to the reactor contained only 0.7% toluene and 2.0% O₂ and therefore constituted a single phase SCF mixture.

The phase diagrams for heavier molecules dissolved in SC-CO₂ indicate that their solubilities in the SCF phase will be much lower than that of toluene. For example the equilibrium mole fraction for phenanthrene in SC-CO₂ or CO₂-air mixtures at 473K and 100 atm was found to be less than 1%. However, the solubilities of either component of a binary solid mixture of aromatic hydrocarbons can be enhanced by up to 300% over its single component solubility (14). In addition, we have shown that by mixing a small amount (less than 10%) of a volatile hydrocarbon such as methanol or toluene with the SC-CO₂ it is also possible to greatly increase the solubilities of heavy aromatic hydrocarbons considered "nonvolatile". For example the solubility of DDT in CO₂ at 100 atm and 313K was shown to increase by more than an order of magnitude in CO₂ containing 6.7% methanol (15). These solubility enhancements due to solute-solute interactions should be sufficient to bring the SC-phase concentration of any aromatic single component or mixture into the typical range for vapor-phase oxidation catalysis, about 1-5 mol%.

Partial Oxidation Catalysis

The results of toluene oxidation experiments in a tubular fixed-bed reactor using an SC feed of CO₂, toluene, and air indicate that strongly acidic catalysts such as H⁺-Y zeolite are inactive, and that, of the many supported metal oxides tested (Co, Mo, Co-Mo, and Ni-W oxides, supported on γ-Al₂O₃), the one whose active component was mostly CoO is the most active and also the most selective for partial oxidation to benzaldehyde and benzoic acid (7). Some results comparing this catalyst to a similar one containing mostly Co₃O₄ are given in Figure 4. The turnover numbers for partial oxidation are in the 10⁻⁷-10⁻⁶/s range, with the reactor operated differentially at conversions less than 2%; these rates are based on moles of total active metal.

The efficacy of the CoO compared to Co₃O₄ was also observed in a recent study of p-xylene oxidation in slurry reactors (16), and is probably a manifestation of the importance of the proper Co²⁺/Co³⁺

ratio in the catalysis (see Figure 1). The observed turnover numbers actually exceed those of previous studies where Co(II) homogeneous catalysts were used in the absence of initiators and electron transfer promoters (as in this work). For example, at 343K the observed turnover number for Co(II) acetate-catalyzed toluene partial oxidation is only $8.3 \times 10^{-8}/s$ in pure acetic acid (17). Although rates as high as 0.01/s have been found at higher temperatures (1,18,19), these were measured in the presence of initiators and electron-transfer promoters such as soluble halides. We can adapt these technological developments to the high pressure process by incorporating such additives in the feed or the catalyst.

Effect of Total Pressure

The relatively high catalyst activities in the SCF oxidation process appear to be the result of a pressure effect. Holding the feed composition constant, we varied the total pressure in the reactor from about 80-140 atm, and observed the changes in the partial oxidation rate given in Figure 5. The more than twofold increase in rate might be explained by the effect of pressure on the concentration-based rate constant, as given by transition-state theory:

$$\left(\frac{\partial \ln k}{\partial P} \right)_{T,x} = - \frac{\Delta V^\ddagger}{RT} + \left(\frac{1-n}{P} \right) \left[1 - \left(\frac{\partial \ln Z}{\partial \ln P} \right)_{T,x} \right] \quad 1)$$

In the equation, ΔV^\ddagger is the difference in partial molar volumes of the activated complex and reactants, n is the molecularity of the reaction, and Z is the compressibility. Although this relation holds only for a single-step reaction, it can be used to roughly estimate the pressure effect here. Detailed calculations (20) using the Peng-Robinson equation of state and assuming a transition state thermodynamically similar to the product benzaldehyde [this assumption was tested for several bimolecular reactions of the type $A + B \rightarrow R$ for which the pressure variation was known, and was found to be adequate (21)] predicted an increase in a second-order rate constant of only about 30% for the pressure range of the data in Figure 5. It appears as if rate constant enhancement is not the most important consideration here.

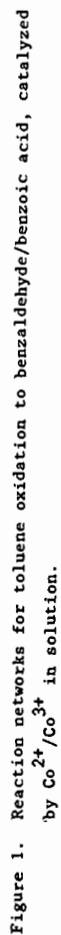
Another possible explanation for the pressure effect is a pressure-dependent variation of O_2 concentration in the condensed "pore" phase of the catalyst. Work with microporous chars and zeolites has indicated that molecules can adsorb in multiple layers in porous media at pressures above the nominal mixture critical pressure, and that the adsorbed phase behaves almost liquid-like in terms of density and heat of adsorption (22,23). Referring to Figure 3, one would expect the capillary pores to be rich in toluene at low pressures but to become enriched in both air and CO_2 at increasing pressures. Because alkylaromatic oxidation reactions are typically of order zero to one in O_2 , pore condensation phenomena could explain the rate increase; this idea is supported by the fact that the rate seemingly levels off near 140 atm, possibly indicating surface saturation.

ACKNOWLEDGEMENT

The work reported here was supported by the Louisiana Center for Energy Studies.

REFERENCES

1. Kaeding, W. W.; Lindblom, R. O.; Temple, R. G.; Mahon, H. I. Ind. Eng. Chem. Process Des. Dev. 1965, 4, 97.
2. Heiba, E. I.; Dessau, R. M.; Koehl, W. J., Jr. Prepr. - Am. Chem. Soc., Div. Pet. Chem. 1969, 14, A44.
3. Kamiya, Y.; Kashima, M. J. Catal. 1972, 25, 326.
4. Sheldon, R. A.; Kochi, J. K. Adv. Catal. 1974, 25, 272.
5. Parshall, G. W., "Homogeneous Catalysis"; Wiley: New York, 1970; Chapters 7 and 10.
6. Schuit, G. C.; Gates, B. C. In "Chemistry and Chemical Engineering of Catalytic Processes"; Prins, R.; Schuit, G. C., Eds.; Sijthoff and Noordhoff, Amsterdam, 1980; p. 461.
7. Dooley, K. M.; Knopf, F. C. Submitted to Ind. Eng. Chem. Research 1986.
8. McMillen, D. F.; Ogier, W. C.; Ross, S. J. Org. Chem. 1981, 46, 3322.
9. Lawson, J. R.; Klein, M. T. Ind. Eng. Chem. Fundam. 1985, 24, 203.
10. Hazlett, R. N.; Solash, J.; Fielding, G. H.; Burnett, J. C. Fuel 1978, 57, 631.
11. King, M. B.; Alderson, D. L.; Fallah, F. H.; Kassim, D. M.; Kassim, K. M.; Sheldon, J. R.; Mahmud, R. S. In "Chemical Engineering at Supercritical Fluid Conditions"; Paulaitis, M. E.; Penninger, J. M.; Gray, R. D., Jr.; Davidson, P., Eds.; Ann Arbor Science: Ann Arbor, MI, 1983; p. 31.
12. Peng, D.-Y.; Robinson, D. B. Ind. Eng. Chem. Fundam. 1976, 15, 59.
13. Heideman, R. A.; Khalil, A. M. AIChE J 1980, 26, 769.
14. Kurnik, R. T.; Reid, R. C. Fluid Phase Equilibria 1982, 8, 93.
15. Dooley, K. M.; Kao, C.-P.; Gambrell, R. P.; Knopf, F. C. Submitted to Ind. Eng. Chem. Research 1986.
16. Hronec, M.; Hrabe, Z. Ind. Eng. Chem. Product Res. Dev. 1986, 25, 257.
17. Zakharov, I. V.; Geletii, Yu. V. Petrol. Chem. USSR 1979, 18, 145.
18. Namie, K.; Harada, T.; Fujii, T. U. S. Patent 3,903,148, 1975.
19. Borgaonkar, H. V.; Raverkar, S. R.; Chandalia, S. B. Ind. Eng. Chem. Product Res. Dev. 1984, 23, 455.
20. Brodt, S. R. M. S. Thesis; Louisiana State University, Baton Rouge, LA, 1987.
21. Dooley, K. M.; Brodt, S. R.; Knopf, F. C. Accepted for publication by Ind. Eng. Chem. Research 1987.
22. Hayhurst, D. T.; Lee, J. C. AIChE Symp. Ser. 1983, 79(230), 67.
23. Jones, M. W.; Isaac, P. J.; Phillips, D. Trans. Faraday Soc. 1959, 1953.



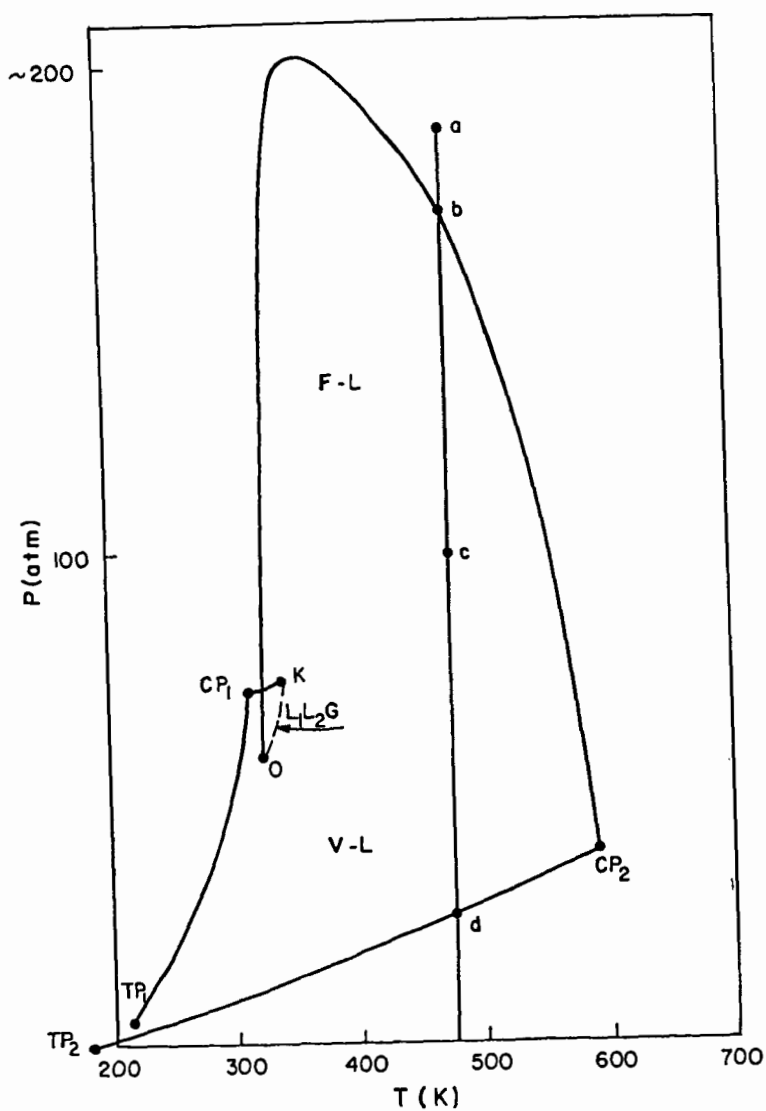


Figure 2. P-T diagram for toluene and CO₂.

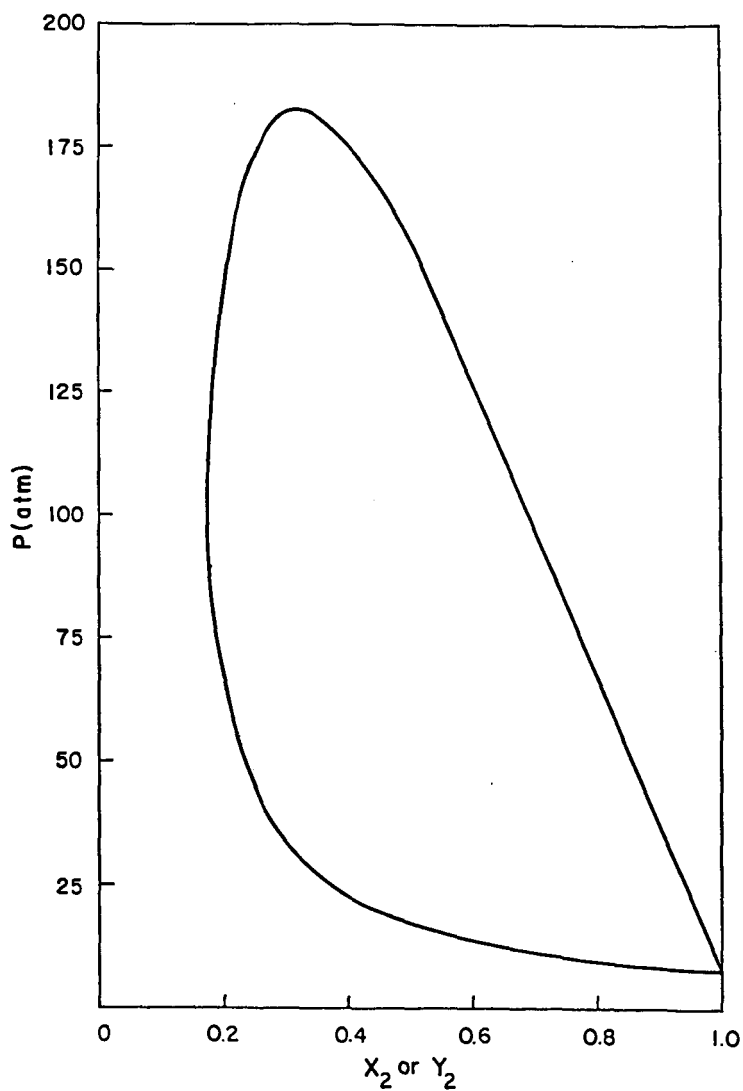


Figure 3. P-X diagram for toluene and CO₂ at 200°C.

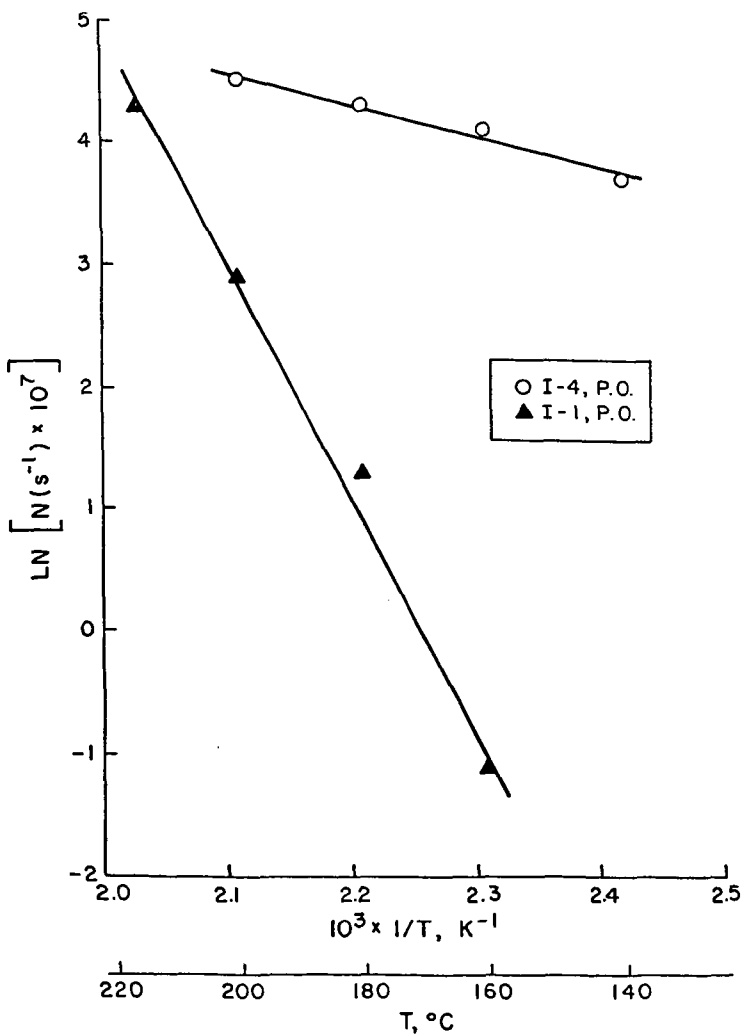


Figure 4. Turnover number for partial oxidation, for two supported Co oxide catalysts calcined at 400°C (I-1) and 200°C (I-4).

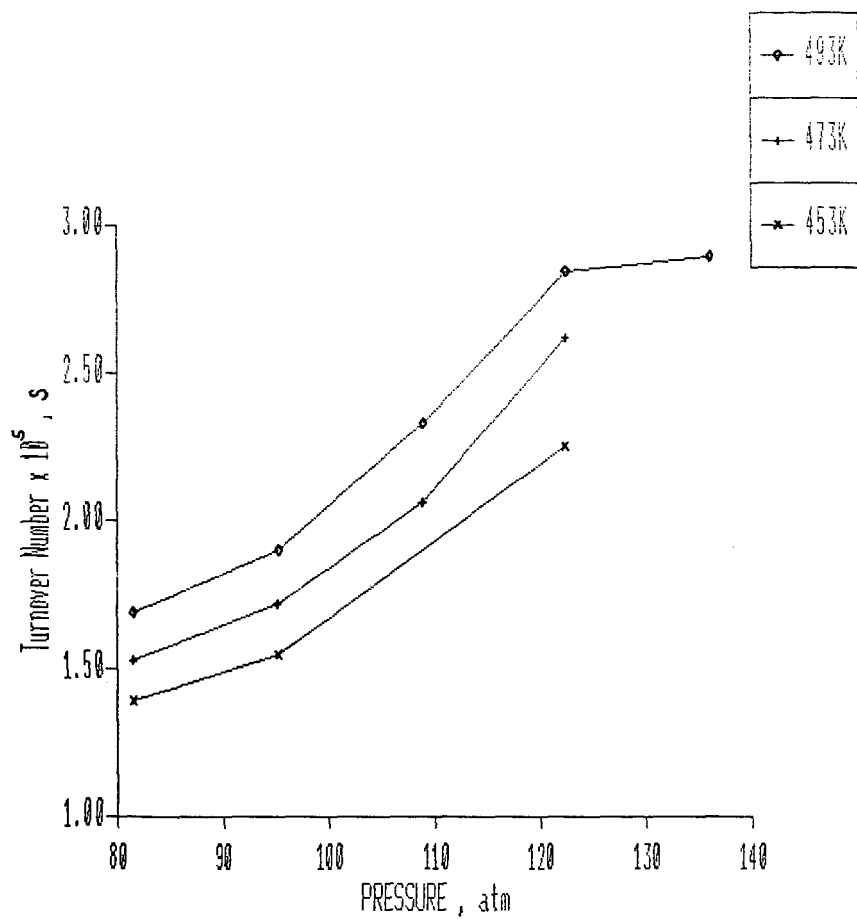


Figure 5. Turnover number per partial oxidation, for a supported Co oxide catalyst calcined at 200°C (catalyst I-4, 5% CoO).

A STUDY ON THE DISTRIBUTION OF VARIOUS CHEMICAL SPECIES IN
DIFFERENT COAL LIQUIDS BY SIZE EXCLUSION CHROMATOGRAPHY -
GAS CHROMATOGRAPHY - MASS SPECTROMETRY

C. V. Philip and R. G. Anthony

Kinetic, Catalysis and Reaction Engineering Laboratory
Department of Chemical Engineering, Texas A&M University
College Station, Texas 77843 - (409)845-3376

INTRODUCTION

Size exclusion chromatography - gas chromatography - mass spectrometry (SEC-GC-MS) is a unique technique which we have developed for coal liquid analysis. Size exclusion chromatography (SEC) separates molecules based on size in a short analysis time. Unlike other chromatographic techniques, SEC does not retain sample species on the column, the analysis time is fixed, and everything loaded onto the column elutes within a fixed time frame. The application of SEC is limited only by the solubility of the sample in a solvent. Since tetrahydrofuran (THF) is a good solvent for coal liquids, the separation of coal liquids by SEC is easily achieved with appropriate columns. Although size exclusion chromatography (SEC) has been used primarily for the separation and characterization of polymers based on molecular size or molecular weight, its use can be extended to the separation of smaller size molecules (1-4). Since coal-derived mixtures have several components of similar sizes, the use of SEC alone does not resolve them for the purpose of identification.

Coal liquids, petroleum crudes, and their distillation cuts have been separated into four or five fractions by SEC. These SEC fractions were analyzed by use of GC (6,7,8). The fraction collection procedure was performed manually, which was inefficient, and susceptible to human error (9,10,11,12,13). A preferred technique is to use a computer controlled fraction collection and subsequent GC-MS analysis technique (14,15,16,17,18). The automated fraction collection followed by injection of the fraction into the GC reduces analysis time, and offers an option for the collection of the desired number of fractions at predetermined time intervals. The manual collection of up to 10 one-ml fractions is also used in order to verify the effectiveness of the automated technique.

Mass spectrometers used to be expensive and complex for routine use as a GC detector. The Ion Trap Detector (ITD, Finnigan) is a low priced mass spectrometer (MS) for capillary chromatography. Three analytical tools - SEC, GC, and ITD - are incorporated into a powerful analytical system for the analysis of complex mixtures such as coal liquids, recycle solvent and anthracene oils. The SEC-GC-MS analysis of Wyodak recycle solvent is used to illustrate the speed and effectiveness of the technique.

EXPERIMENTAL

The low rank coals used in the liquefaction experiments were Texas Big Brown lignite from the Wilcox formation, Zap-2 Indian Head lignite and Beulah lignite from North Dakota and Wyodak coal from Wyoming. Mini reactors (6.3 and 20 ml) used mostly Autoclave high pressure fittings (11). The liquefaction solvents included anthracene oil, four recycle solvents from the coal liquefaction pilot plant at the University of North Dakota Energy Research Center (UNDERC) and water under supercritical conditions. Hydrogen, carbon monoxide and hydrogen sulphide were the reactive gases which were used in varying proportions (19). The samples of liquid products from selected

experimental conditions were used for the detailed analysis.

The product slurry as well as the recycle solvents were extracted with tetrahydrofuran (THF) and the solubles were used as samples for the analysis. The technique for the analysis is based on the integrated use of three instruments - a size exclusion chromatograph (SEC) with a 100Å SEC column, a high resolution gas chromatograph with a bonded phase wide bore fused silica column and an Ion Trap Detector (ITD, Finnigan), a mass spectrometer for capillary chromatograph (Figure 1). A sample injected into the SEC was separated based on linear molecular size and the fractions of effluents were collected at preprogrammed time intervals. The SEC-GC interface is illustrated in Figure 2. The separation of each fraction is continued on the capillary column and the components were detected by the mass spectrometer (ITD). The mass spectral fragmentation data were stored on a 10 megabyte hard disk and were later analyzed by the library search using National Bureau of Standards (NBS) mass spectral data base which has fragmentation patterns of about 40,000 organic compounds. The library search was used to identify the general formula as well as probable functional groups of most major components in coal liquids. The identification of each species was achieved by using several factors including SEC retention volume (linear molecular size), GC retention time (boiling point, molecular weight) and mass spectral fragmentation pattern. Since the coal liquids contain many components, the mass spectral data of some compounds were not available in the library. A very careful evaluation of the MS fragmentation pattern was necessary to establish the identity of the compound. Identification of unknowns needed better MS fragmentation pattern and time. Once a compound was identified, the information was continuously used for identifying trace amounts based on masses of the major fragments.

RESULTS & DISCUSSION

Analysis of Wyodak recycle solvent

The detailed discussion of SEC-GC-MS analysis Wyodak recycle solvent can be used to illustrate the analysis technique as well as the composition of coal liquids. Wyodak recycle solvent contains some anthracene oil distillate as well as coal depolymerization products stabilized by the liquefaction conditions. Figure 3 shows the SEC separation of Wyodak recycle solvent. The separation pattern of various chemical species and chemical groups are assigned based on reported (4-15) as well as unreported studies. When valves V_2 and V_3 (Figure 2) are engaged, the SEC effluents are collected in the sample loops of V_3 at specific intervals. The refractive index detector output shows the effect of such fraction collections as negative peaks (Figure 4). Sixteen SEC fractions of 100 μ l each were collected from the Wyodak recycle solvent (Figure 4) at 0.5 min intervals. Each fraction was analyzed by injecting 0.1 μ l into the GC, which used the flame ionization detector (FID). The first three fractions and the last fraction showed the GC of the solvent; so the GC of those fractions are not included in Figure 5. The first GC (Figure 5.1) corresponds to the GC of fraction #4 and the last GC (Figure 5.12) is that of fraction #15. By increasing the GC oven temperature the larger alkanes in fraction #2 and #3 can be detected. A shorter column enhances the FID response as these heavy alkanes accumulate on the column probably due to irreversible adsorption or decomposition.

Figure 5.1 shows the GC of fraction #4. It shows alkanes ranging from C_{25} to C_{30} . It is quite possible that the fraction may contain higher alkanes which are not detected due to the GC-oven temperature limit. The peaks are identified from the MS fragmentation pattern. Fraction #5 is collected after a 0.5 minute interval and its GC (Figure 5.2) shows alkanes ranging from C_{19} to C_{30} . This fraction has lower alkanes (C_{19} - C_{24}) in larger proportions in addition to smaller amounts of alkanes

(C₂₅-C₃₀) which were detected earlier in fraction #4. The peak due to C₂₇ is larger relatively to other alkanes in Figure 5.1 and 5.2. Our experience with fossil fuels indicates that the straight chain alkanes (n-alkanes) have a normal distribution over a wide molecular weight range. Even in other reported works on hydrocarbon fuels an unusual enhancement of a particular straight chain alkane is not observed. The alkane fractions always contain branched alkanes such as pristane, phytane, and hopane, and some of them are called biological markers. It is quite possible that the C₂₇ peak could be due to some branched alkanes co-eluting with n-C₂₇.

The GC of fraction #6 is shown in Figure 5.3, which contains mostly alkanes in the range of C₁₅-C₂₄ and small amounts of C₁₄ and C₂₅-C₂₉. The fraction #6 was collected 0.5 minute after fraction #5 and one minute after fraction #4. If fraction #5 had not been collected, the GC of fraction #4 and #6 which were one minute apart could have been used to qualitatively, but not necessarily quantitatively, determine all of the species. Fraction #5 has species from both fractions #4 and #6. The peak width of species eluting at these retention times is about one minute. Hence SEC fraction collection at one min (one ml) intervals would have contained all the species with less overlapping and analysis time could have been reduced to half. A short peak immediately after C₁₇ is pristane (trimethylhexadecane). The short peaks that appear between the n-alkane peaks appear to be isoalkanes or branched alkanes. The baseline appears to be shifted slightly upward compared to the baseline of the GC's in Figure 5.1 and 5.2. This is probably due to a large number of possible isomers of phenolic species. GC of fraction #7 (Figure 5.4) has alkanes as small as C₁₂. The ratio of peak heights of pristane to C₁₇ increases in the GC of this fraction compared to previous fractions as expected from its shorter linear molecular size. The smaller peaks between n-alkane peaks are alkylated phenols and branched alkanes.

Fraction #8 (Figure 5.5) is mostly alkylated phenols and indanols with a trace amount of smaller alkanes. The baseline shift is due to the co-elution of several large phenolic species in many isomeric forms. Fraction #9 (Figure 5.6) does not contain any alkanes. The ratio of the o-cresols to m-, p-cresols increases from fraction #8 to #9. Both m-cresol and p-cresol are structurally longer than o-cresol. Some long aromatic species such as biphenyls also appear in this fraction. Compared to fraction #8, the phenols in fraction #9 are of shorter size while the peaks appearing at long GC retention times are aromatics. It is safe to say that phenols appear before 16 minutes of GC retention time followed by aromatics after 16 minutes. The GC of fraction #10 is shown in Figure 5.7. Light phenols including xylanols and cresols present in this fraction are separated on the GC before a retention time of 8 minutes. The species appearing after 8 minutes are aromatics, mostly with alkyl side chains.

Fraction #11, whose GC is in Figure 5.8, contains phenol, which appears at 3 minutes. Phenol is the only phenolic in Fraction 11. Almost all possible isomers of one and two ring aromatics with alkyl side chains (propyl or shorter) are detected in this fraction. Since the number of species are higher, co-elutions of two or more components at one GC retention time is observed. The mass spectral fragmentation pattern can be used to assign the molecular formula and general structural nature. The identification of isomers is very difficult in a number of cases. The NBS Mass Spectral Data Base has only a fraction of the needed standard reference spectra to identify the species in this fraction. Most of the identification has been assigned based on the fragmentation patterns and boiling points derived from the GC retention times. Fraction #12 as shown in Figure 5.9 has overlapping from two types of aromatics - alkylated aromatics and polycyclic aromatics. Fraction #13 contains aromatics

with slight alkylation and the ring numbers increase as shown in Figure 5.10. Both fractions #14 and #15 (Figure 5.11, 5.12) contain only multi-ring aromatics with few alkyl side chains. One exception to the rule that SEC separates species in decreasing order of linear molecular size is that condensed ring aromatics tend to remain in the column longer. Some polycyclic aromatics such as pyrene and coronene are eluted from the gel column only after naphthalene although they are much larger. More pyrene is in Fraction #15 than in Fraction #14 but the reverse is true for anthracene which appears before naphthalene.

Distribution of Alkanes in Coal Liquids

One of the major results of SEC-GC-MS studies is the discovery of an orderly pattern, by which various isomers and homologs of similar chemical species exist in coal liquids. For example almost any direct coal liquefaction process produces very similar species which differ from each other by size and extent of isomerization but with an orderly distribution pattern. Alkanes ranging from $C_{12}H_{26}$ and $C_{44}H_{90}$ are detected in almost any coal liquid. Most of these are straight chain alkanes showing an orderly continuous pattern. Neither is a particular n-alkane almost absent nor is it present in a disproportionate amount. Exceptions exist for some branched alkanes such as pristane, phytane, and hopane. These species are also called biomarkers and their concentration varies depending on the sample. The straight chain hydrocarbons, mainly the alkanes, are observed as sharp GC peaks in the GC of certain SEC fractions of lignite-derived liquids. The corresponding SEC-fractions of the anthracene oil show a "hump" in the GC. It appears that the pyrolytic conditions used in a coking oven are destroying or converting most of the straight-chain alkane species into numerous isomeric hydrocarbons. The MS fragmentation patterns of the GC "hump", are similar to that of alkanes.

Distribution of Phenols in Coal Liquids

Phenols are a major chemical lump present in coal liquids. Phenols have basically one or more aromatic ring structures with alkyl substituents. Methyl, ethyl and propyl are the most common alkyl substituents. The smallest species is the one with a hydroxyl group attached to a benzene ring. Addition of a methyl group produces three isomers - o-, m-, and p-cresols. It appears that all three are present in about the same proportion. The number of possible isomers increases as the possible number and size of alkyl substituents increases. It is expected that higher degree of alkylation can produce larger molecules in a larger number of isomeric forms, separation of which is rather difficult even by high resolution GC methods. This could be the reason why a shift in the GC baseline is observed for the SEC phenolic fractions rather than resolved peaks. Since these shifts are quite reproducible and real, it can be assumed that these "bumps" are due to a large number of components eluting continuously without resolution. Their SEC retention time suggests that they are probably phenols. The gas chromatographers who are used to fewer sharp peaks from capillary GC may prefer to resolve them. Sometimes derivatization techniques are used to obtain sharper well resolved peaks. As a matter of fact unresolved "bumps" are telling a story. Too many isomers of close molecular weight or boiling point are eluting without resolution at close retention times. Phenols do show peak tailing in most GC separation conditions. But currently available capillary columns do not show tailing as a serious problem. Peak tailing is expected to decrease as the degree of alkylation increases. Peak tailing for cresol is less than that for phenol. It is much improved for xylenols. The derivatization of phenols prior to GC separation may produce fewer well-resolved peaks but at the expense of losing some components.

Distribution of Aromatics in Coal Liquids

The number of isomers of alkylated aromatics is enormous. Lower members of alkylated benzenes such as xylenes are well-resolved and detected by FID and MS. Increased alkylation causes an increase in the number of isomers. In the case of both alkylated phenols and aromatics various isomers exist in a continuous pattern. The less alkylation gives few well-resolved isomers. The more alkylation gives a large number of isomers but in smaller concentrations.

We have observed a striking similarity in the identity of chemical species found in different types of coal liquids such as anthracene oil (A04), recycle solvents and the lignite-derived liquids from our liquefaction experiments as they are separated by SEC-GC and identified by MS. The polycyclic aromatic species which are characteristic of coking oven products from coal, such as anthracene oil and creosote oil are found in all lignite-derived liquids from our liquefaction experiments, including the liquid obtained by the dissolution of lignite in water under super critical conditions. Their relative concentration was found to increase varying with the severity which is used to produce the coal liquid. Anthracene oil has the highest concentration of polycyclic aromatics and the lignite liquefied in supercritical water has the lowest. The hydroxy aromatics, also known as alkylated phenols, which are produced under lignite liquefaction experiments, are not major components in anthracene oil.

CONCLUSIONS

The coal conversion products are compounds of at least two types of species. "a" The species which are released from the coal matrix and stabilized by the coal liquefaction process. This type of species retains most of its original structural characteristics. Most of the alkanes and alkylated phenols belong to this group. "b" The species which are characteristic of high temperature reactions. The polycyclic aromatics such as phenanthrene and pyrenes are products of high temperature chemistry. Coke ovens and even wood burning fireplaces produce these products. The liquefaction environment can cause additions of alkyl side chains to these species although higher temperature causes the dealkylation of these products. Some of these species may be existing in coal but in lower concentrations.

The coal liquefaction process generates both types of compounds. Lower temperatures favor type "a" compounds while higher temperatures tend to produce more of type "b" compounds. The SEC-GC-MS analysis data on a number of coal liquids produced under varying conditions from different coals and liquefaction solvents indicate that liquefaction temperatures below 400°C produce very little type "b" compounds although they are not totally absent. The alkylated aromatics such as alkyl indans and benzenes appear to be generated from the original coal structure although these compounds could be catatytically generated at these temperatures even from simple starting materials such as CO and H₂. Several low temperature reactions products from coal support the existence of one or two ring aromatics with other substituents, especially in low rank coals.

ACKNOWLEDGEMENTS

The financial support of the U.S. Department of Energy, (project Number DE-AC18-83FC10601), Texas A&M University Center for Energy and Mineral Resources and Texas Engineering Experiment Station is gratefully acknowledged. The Energy Research Center at University of North Dakota furnished samples for the study.

REFERENCES

1. Hendrickson, J.G., "Molecular Size Analysis Using Gel Permeation Chromatography",

- Anal. Chem.*, 1968, 40, 49.
2. Majors, R.E.J., "Recent Advances In HPLC Packing and Columns", *Chromatog. Sci.*, 1980, 18, 488.
3. Cazes, J. and D.R. Gaskill, "Gel-permeation Chromatographic Observation of Solvent-solute Interaction of Low-molecular Weight Compounds", *Sep. Sci.*, 1969 4, 15.
4. Krishen, A. and R.G. Tucker, "Gel-permeation Chromatography of Low Molecular Weight Materials With High Efficiency Columns", *Anal. Chem.*, 1977 49, 898.
5. Philip, C.V., Anthony, R.G., "Dissolution of Texas Lignite in Tetralin", *Fuel Processing Technology*, 1980, 3, p. 285.
6. Zingaro, R.A., Philip, C.V., Anthony, R.G., Vindiola, A., "Liquid Sulphur Dioxide - A Reagent for the Separation of Coal Liquids", *Fuel Processing Technology*, 1981, 4, 169.
7. Philip, C.V., Zingaro, R.A., Anthony, R.G., "Liquid Sulfur Dioxide - as an Agent for Upgrading Coal Liquid", "Upgrading of Coal Liquids," Ed. Sullivan, R.F., *ACS Symposium Series No. 156*, 1981;p.239.
8. Philip, C.V., Anthony, R.G., "Chemistry of Texas Lignite Liquefaction in a Hydrogen-donor Solvent System", *Fuel*, 1982, 61, 351.
9. Philip, C.V., Anthony, R.G., "Separation of Coal-derived Liquids by Gel Permeation Chromatography", *Fuel*, 1982, 61, 357.
10. Philip, C.V. and Anthony, R.G., "Analysis of Petroleum Crude and Distillates by Gel Permeation Chromatography (GPC)", "Size Exclusion Chromatography", Ed. Proudler, T., *ACS Symp. Series*, 1984, 245, 257.
11. Philip, C.V., Anthony, R.G. and Cui, Z.D., "Structure and Reactivity of Texas Lignite", "Chemistry of Low-Rank Coals, Ed. Schobert, H.H., *ACS Symp. Series*, 1984, 264, 287.
12. Philip, C.V., Bullin, J.A. and Anthony, R.G., "GPC Characterization for Assessing Compatibility Problems with Heavy Fuel Oils", *Fuel Processing Technology*, 1984, 9, 189.
13. Sheu, Y.H.E., Philip, C.V., Anthony, R.G. and Soltes, E.J., "Separation of Functionalities in Pyrolytic Tas by Gel Permeation Chromatography", *Chromatographic Science*, 1984, 22, 497.
14. Philip, C.V. and Anthony, R.G. "Separation of Coal Liquids by Size Exclusion Chromatography - Gas Chromatography (SEC-GC)", *Am. Chem. Soc. Div. Fuel Chem. Preprints*, 1985, 30, (1), 147.
15. Philip, C.V. and Anthony, R.G. "Characterization of chemical Species in Coal Liquids Using Automated Size Exclusion Chromatography - Gas Chromatography (SEC-GC)", *Am. Chem. Soc. Div. Fuel. Chem. Preprints*, 1985, 30 (4), 58.
16. Philip, C.V. and Anthony, R.G. "Separation of Coal Liquids by Size Exclusion Chromatography - Gas Chromatography (SEC-GC)", *Journal of Chromatographic Science*, 1986, 24 (10), 438.
17. Philip, C.V. and Anthony, R.G. "Gel Permeation Chromatography - Gas Chromatography - Mass Spectrometry (GPC-GC-MS) Instrumentation for the Analysis of Complex Samples", Pittsburgh Conference Atlantic City March 9-13, 1987, paper #788.
18. Philip, C.V., Moore, P.K., and Anthony, R.G. "Analysis of Coal Liquids by Size Exclusion Chromatography - Gas Chromatography - Mass Spectrometry (SEC-GC-MS)", accepted for publication in *Advances in Size Exclusion Chromatography*, *ACS Symposium Series*, 1987.
19. Anthony, R.G., Philip, C.V. and Moore P.K. "Kinetic Model Development for Low-Rank Coal Liquefaction", Final Technical Report for Low Rank Coal Liquefaction, March 15, 1983 - October 31, 1986, DOE/FC/1060-13.

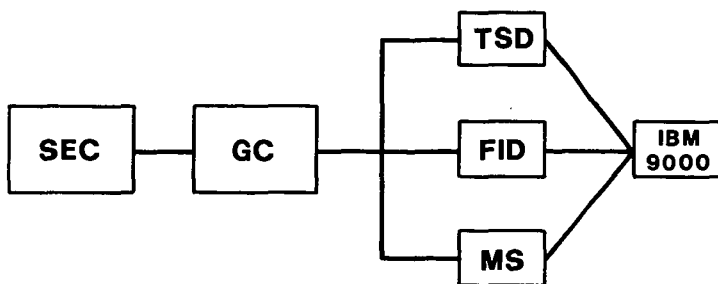


Figure 1. SEC-GC-MS instrumentation.

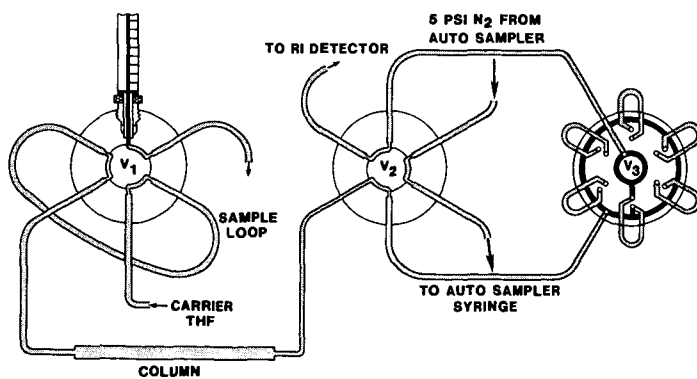


Figure 2. SEC-GC interface Note: V_3 has sixteen sample loops instead of six shown.

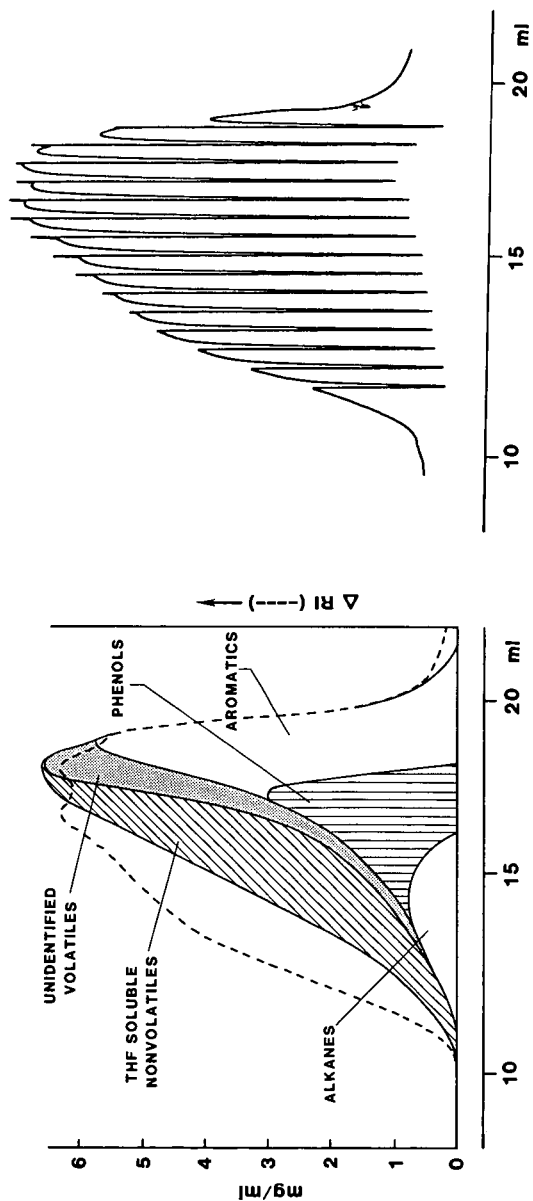


Figure 3. SEC of Wyodak recycle solvent.

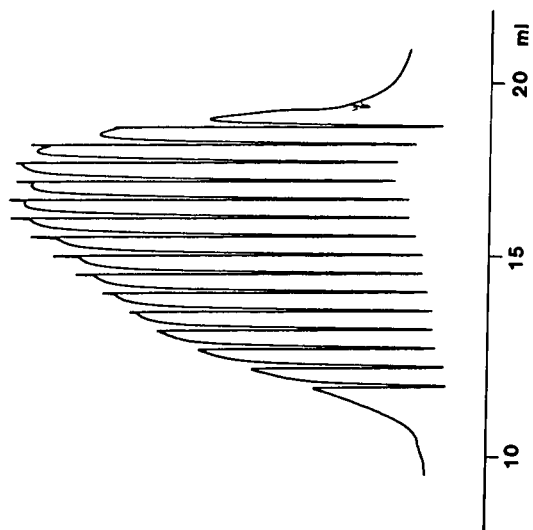


Figure 4. 100 μ l fractions collected by SEC-GC interface (on-line).

SEC-GC-MS OF WYODAK RE-CYCLE SOLVENT

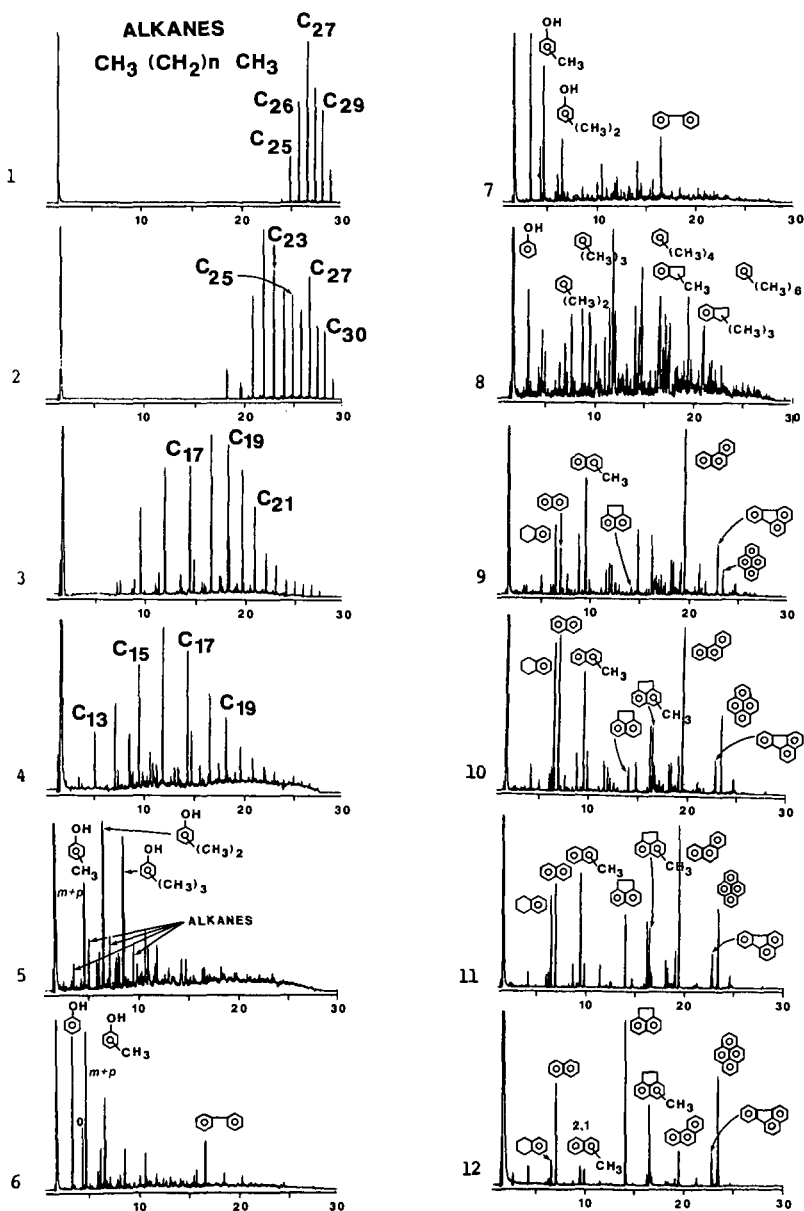


Figure 5. SEC-GC-MS of Wyodak re-cycle solvent.

THE HYDROGEN TRANSFER CYCLE FOR COAL LIQUEFACTION -- PROCESS IMPLICATIONS*

H. P. Stephens and R. J. Kottenstette
Sandia National Laboratories, Albuquerque, NM 87185

INTRODUCTION

Direct liquefaction of coal involves the conversion of a hydrogen-poor solid to a liquid richer in hydrogen by a complex set of bond ruptures and hydrogen transfer reactions. This paper reports a portion of a continuing effort to understand the utilization of hydrogen in direct liquefaction by tracing the transfer of hydrogen from the gas phase to polynuclear aromatic hydrocarbon (PAH) solvent components, and from these donor components to coal. In this portion of the effort, experiments were performed to monitor the dehydrogenation of hydroaromatic components of a coal-derived solvent that results from donation of hydrogen to coal.

In a previous paper (1), results of experiments were reported that showed the impact of a hydrogen source, either from the gas phase or from solvent containing hydroaromatic compounds, on the yield of liquefaction products. Gas-phase hydrogen was required to produce high conversion of coal to liquids only if the solvent contained low concentrations of hydroaromatic donors. Furthermore, significant consumption of gas-phase hydrogen occurred only in reactions catalyzed to promote in-situ hydrogenation of PAHs to hydroaromatics. In related experiments (2,3,4), we have sought to define effective conditions for the hydrogenation of PAHs in coal-derived solvents. The results of these studies demonstrated that 1) use of catalytic hydrogenation at relatively low temperatures favored formation of hydroaromatics; 2) use of lower temperature allows the use of lower pressure; and 3) that CO/water mixtures are effective sources of hydrogen for hydrogenation of PAHs. These results were used to establish conditions for preparing a liquefaction solvent containing high concentrations of hydroaromatic hydrogen donors. This solvent was then reacted with coal, in the absence of gas-phase hydrogen, over a range of temperatures and times to monitor the transfer of hydrogen from the hydroaromatic derivatives of three key PAHs, phenanthrene, fluoranthene, and pyrene.

EXPERIMENTAL

Materials

Feed to the solvent production reactor was prepared from a pasting solvent produced from Illinois No. 6 (Burning Star) coal by the Lummus Integrated Two-Stage Liquefaction (ITSL) process development unit (5). This material, which was too viscous to be used in our laboratory reactor, had a boiling point range of approximately 550 to 850°F. Prior to its use, it was vacuum distilled with a spinning band apparatus. The 650 to 770°F fraction, which contained 3.3% by weight phenanthrene, 4.0%

* This work supported by the U.S. Department of Energy at Sandia National Laboratories under Contract DE-AC04-76DP00789.

fluoranthene and 8.6% pyrene, was retained for these experiments. Illinois No. 6 high-volatile bituminous coal for these experiments was obtained from the Argonne National Laboratory Premium Coal Sample Program. The coal was found to have 7.3% by weight moisture and 17.5% mineral matter by low temperature ashing. Extrudates (0.8 mm diameter by 4 mm length) of Shell 324M, a 2.8% Ni, 12.4% Mo on alumina catalyst, were used for hydrogenation of the solvent. Prior to use, the catalyst was sulfided in situ with 10 mole % H_2S in H_2 at 390°C and atmospheric pressure.

Apparatus and Procedure

Solvent hydrogenation was performed in a trickle-bed reactor using steam and a 1:1 "syngas" mixture of hydrogen and carbon monoxide to simulate the products of a gasifier. The reactor consisted of six 1.0 cm ID by 15 cm long catalyst-filled stainless steel tubes connected in series. Each tube contained 9.5 g of catalyst. The reactor was thermostatted to $\pm 1.0^\circ C$ by a forced-air convection oven and pressure was controlled to ± 10 psig with a precision back pressure regulator. After pressurizing to 800 psig with the gas mixture, the reactor temperature was brought to 300°C and water flow was initiated. Upon detection of conversion of CO/H_2O to CO_2/H_2 , the coal-derived solvent flow was started. The gas mixture was delivered to the reactor at a volume hourly space velocity of 325 and steam and solvent were delivered at weight hourly space velocities of 0.07 and 0.5 respectively. The amount of steam fed to the reactor was slightly in excess of the amount required to stoichiometrically convert all of the CO. During the operation of the reactor, 0.5 mole % of H_2S was added to the gaseous feed to maintain the catalyst in the sulfided state.

Coal liquefaction reactions were performed in batch microautoclaves with slurry capacities of 8 cm³ and gas volumes of 35 cm³ (6). After the reactors were charged with 8g of a 2:1 ratio mixture of solvent and coal, they were pressurized to 300 psig with nitrogen. They were then heated to temperature in a fluidized sand bath while being agitated with a wrist-action shaker at 200 cycles/min. Following the heating period, the reaction vessels were quenched in water, the final temperatures and pressures were recorded, a gas sample was taken and the product slurry was quantitatively removed for analysis. All experimental variables for both the flow and batch reactors were monitored and recorded with a computer-controlled data acquisition system. Four coal liquefaction experiments were performed to correlate dehydration of the hydroaromatics with coal conversion. Reactions were performed at two temperatures, 425 and 450°C, and for times ranging from 10 to 40 minutes.

Product Analyses

Gas samples from the liquefaction reactions were analyzed for N_2 , H_2 , CO, CO_2 , and C_1 - C_3 hydrocarbons with a Carle Series 500 gas chromatograph with a hydrogen transfer system. The amounts of PAHs and hydroaromatics in the flow reactor feed and liquid product samples were determined with a Hewlett-Packard 5890 gas liquid chromatograph equipped with a capillary column. Coupled gas chromatography/mass spectrometry techniques were used to

identify the retention times of the PAHs and hydrogenated PAHs. Hydrogen content of the product was determined by elemental analysis. To calculate the amount of donatable hydroaromatic hydrogen, a portion of the coal-derived solvent that was catalytically dehydrogenated was also analyzed for hydrogen content. Conversion of coal to products was quantified by tetrahydrofuran (THF) and n-heptane solubility. Dry, mineral matter free (dmmf) basis conversions were calculated from the difference between the weight of organic coal and the insoluble organic matter resulting from THF or n-heptane extraction of the product. The n-heptane soluble materials, which contained the post-reaction solvent components, were examined by capillary column chromatography to determine the extent of dehydrogenation of solvent hydroaromatics.

RESULTS AND DISCUSSION

Solvent Hydrogenation

The extent of solvent hydrogenation can be seen in Figure 1, which is a comparison of the chromatogram of the trickle-bed reactor product to that of the feed. Analysis of the product solvent showed that 66% of the phenanthrene, 88% of the fluorene and 56% of the pyrene were converted to hydroaromatics. Table I gives the concentrations and distribution of the hydroaromatics resulting from hydrogenation of the PAHs. It was also noted from the chromatograms that the solvent contained significant amounts of alkylated phenanthrenes and pyrenes, which were also hydrogenated. However, the concentrations of these were not quantified. From the difference between the hydrogen content of the solvent (9.0%) and that of a catalytically dehydrogenated sample (8.2%), the donatable hydrogen content was calculated to be 0.8% by weight.

Coal Liquefaction and Hydrogen Donation

Table II presents a summary of the results of the coal liquefaction experiments in terms of insoluble organic material (IOM) remaining after reaction, n-heptane insoluble and soluble products formed, yield of hydrocarbon gases (C_1 - C_3) and release of hydrogen to the gas phase. As can be seen from Table II, the highest reaction severity, 450°C for 40 minutes, produced a significant conversion of coal to n-heptane soluble products (44%) with only a small amount (16%) of hydrogen released to the gas-phase.

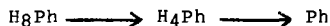
Figures 2-4 trace the concentrations of the PAHs and hydroaromatics as a function of conversion of coal to the sum of the yields of n-heptane soluble materials and hydrocarbon gases. Several observations can be made with respect to hydrogen donation by the hydroaromatic species.

Comparison of the PAH and hydroaromatic concentrations resulting from experiments 2 and 3 shows that the extent of donation is directly proportional to conversion of coal to products. Though experiments 2 and 3 were performed for different times and at different temperatures, the product distributions were

nearly identical, as were the post-reaction concentrations of PAHs and hydroaromatic solvent components.

Examination of the concentration curves shown in Figures 2-4 indicates the relative ease with which the various hydroaromatics donate hydrogen during the conversion of coal. Three groups of hydroaromatics can be distinguished: First are those which donate early in the coal conversion process, as indicated by sharply decreasing concentrations at the lowest coal conversion. Tetrahydrofluoranthene, di-, tetra- and 1,2,3,6,7,8-hexahydropyrene can be placed in this group. The second group consists of hydroaromatics that donate later in the coal conversion process, as indicated by sharply declining concentrations at higher conversions. Tetrahydrophenanthrene, hexahydrofluoranthene and decahydrofluoranthene belong to this group. The third group are hydroaromatics that show a steady decrease in concentration over the entire range of coal conversion. Three compounds, dihydrophenanthrene, octahydrophenanthrene, and 1,2,3,3a,4,5-hexahydropyrene (isohexahydropyrene in Fig. 4) exhibit this behavior.

Examination of the concentration profiles for the hydrophenanthrenes indicates the existence of a multiple step donation for octahydrophenanthrene. Initially, as the concentration of octahydrophenanthrene (H_8Ph) decreases, the concentration of tetrahydrophenanthrene (H_4Ph) increases. The concentration of H_4Ph does not decrease much until the concentration of H_8Ph is substantially lower. This is consistent with the following dehydrogenation pathway which results from hydrogen donation:



Implications for Coal Liquefaction Processes

This study of the hydrogen transfer cycle for coal liquefaction suggests more effective ways to utilize hydrogen. The results of these experiments clearly demonstrate that an excellent coal liquefaction solvent can be produced by reaction of a coal-derived liquid with a H_2/CO /steam mixture at relatively low temperature and pressure. The resulting solvent contains a sufficient concentration of hydroaromatics to be used as the sole source of hydrogen for the liquefaction of coal. Applying these techniques for transfer of hydrogen to coal in a liquefaction process could provide several advantages: First, use of CO/H_2 /steam mixtures, instead of purified hydrogen, for the hydrogenation of the solvent would eliminate the need for gas purification units. Second, operation of the solvent production reactor at a lower temperature and pressure would allow reduction of the wall thickness of the reactor vessel, thus reducing vessel cost. Third, the 650-770°F distillate cut used as a recycle solvent contains significant concentrations of the important three- and four-ring hydroaromatic donor precursors, but does not contain compounds that cause extensive catalyst deactivation. Finally, the requirement for gas-phase hydrogen and high pressure in the thermal liquefaction step would be eliminated.

REFERENCES

1. H. P. Stephens, Proceedings of the 1983 International Conference Coal Science, Pittsburgh, PA, August 1983, p. 105.
2. H. P. Stephens and R. J. Kottenstette, Preprint of Papers, American Chemical Society, Fuel Division, Vol. 30, No. 2, 345, April 1985.
3. H. P. Stephens, Proceedings of the 1985 International Conference on Coal Science, Sydney, Australia, October 1985, p. 327.
4. H. P. Stephens, Preprint of Papers, American Chemical Society, Fuel Division, Vol. 31, No. 4, 314, September 1986.
5. H. D. Schindler, J. M. Chen, and M. Peluso, Proceedings of the Seventh Annual EPRI Contractors' Conference on Coal Liquefaction, p. 2-1, EPRI AP-2718, Palo Alto, CA, November 1982.
6. R. J. Kottenstette, Sandia National Laboratories Report SAND82-2495, 6 (1983).

TABLE I Distribution of phenanthrene, fluoranthene, pyrene and hydroaromatic derivatives in hydrogenated coal-derived solvent.

Compound	Conc. in Solvent (Wt %)	Percent of PAH Mixture
Phenanthrene	1.03	34
9,10-dihydro-	0.38	13
1,2,3,4-tetrahydro-	0.79	26
1,2,3,4,5,6,7,8-octahydro-	0.81	27
Fluoranthene	0.51	12
1,2,3,10b-tetrahydro	1.96	46
6b,7,8,9,10,10a-hexahydro-	0.71	17
1,2,3,3a,6b,7,8,9,10,10a-decahydro-	1.06	25
1,2,3,3a,4,5,6,6a,10b,10c-decahydro-		
Pyrene	3.81	44
4,5-dihydro-	2.49	29
4,5,9,10-tetrahydro-	0.53	6
1,2,3,6,7,8-hexahydro-	0.98	11
1,2,3,3a,4,5-hexahydro-	0.77	9

TABLE II Summary of Results of Coal Liquefaction Experiments

Exp. No.	Temp (°C)	Time (min.)	Product Distribution (% dmmf coal basis)				Hydrogen Released to Gas Phase (% of donatable hydrogen)
			10M	Hept. Sol.	Hept. Insol.	C ₁ -C ₃	
1	425	10	9.5	22.4	66.9	0.8	3.9
2	425	30	6.7	36.3	54.5	1.5	6.9
3	450	10	6.8	36.3	53.3	2.5	7.5
4	450	40	4.1	43.5	45.9	6.4	16.1

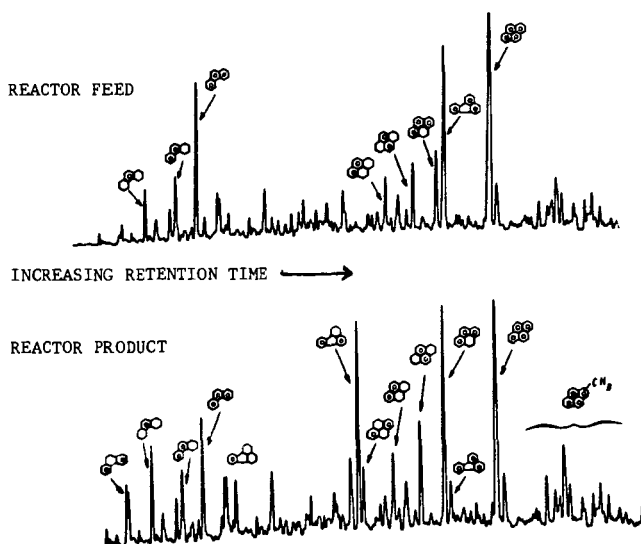


FIGURE 1. Comparison of Chromatograms of Trickle Bed Reactor Feed and Product

Fig. 2. Concentration of phenanthrene and hydrophenanthrenes vs coal conversion.

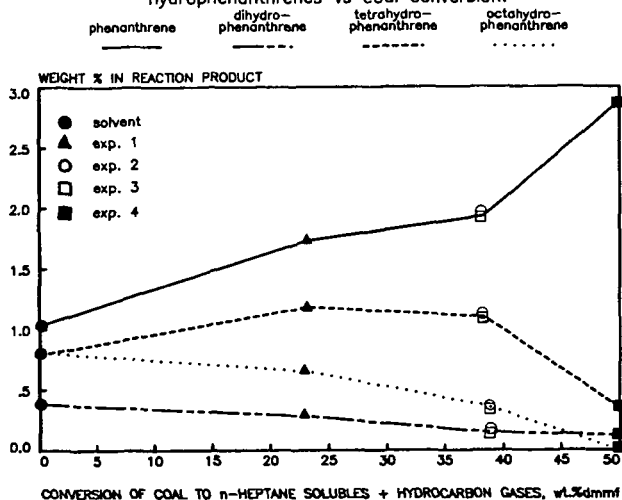


Fig. 3. Concentration of fluoranthene and hydrofluoranthenes vs coal conversion.

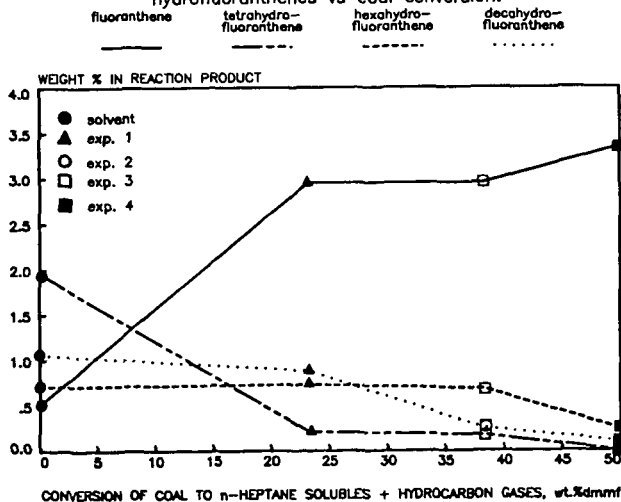
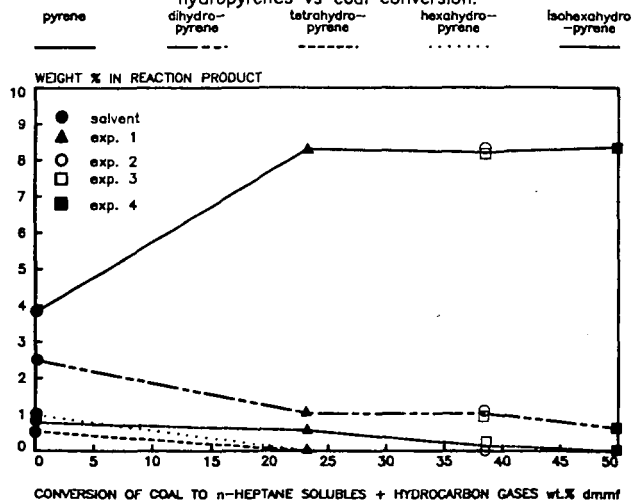


Fig. 4. Concentration of pyrene and
hydropyrenes vs coal conversion.



Investigation on the Nature of Steam Modified Coal

S.D. Brandes and R.A. Graff

The Clean Fuels Institute, The City College of New York
New York, New York 10031

Introduction

In previous work it was found that dramatically improved liquid yields from steam pyrolysis and mild solvent extraction of bituminous coal are obtained when the coal is first exposed to subcritical steam for short periods of time (Graff and Brandes, 1984 and 1987). This finding motivated the investigation, reported here, into the nature of coal after modification by subcritical steam.

In this work solvent swelling, a technique to determine the degree of cross-linking between macromolecular units in coal (Green, et al. 1984), has been applied. An estimate of the degree of hydrogen bonding in the coal was thereby obtained.

Treated coal was also analyzed by diffuse reflectance infrared spectroscopy (DRIS) and by an o-alkylation procedure described by Liotta (1981). The results of these three studies are described in this paper.

EXPERIMENTAL PROCEDURES

Tests were conducted using a batch of Illinois No.6 coal¹ ground under an inert atmosphere to pass 200 mesh and having the following elemental analysis (wt%, maf) : 76.1 C, 5.3 H, 1.3 N, 5.1 S, 11.8 O.²

Treatment

Treatments of coal samples were carried out in a series of fixed bed reactors. The reactors are constructed from lengths of stainless steel tubing (2.54cm X 1.35cm). The length of the tube was varied to accommodate different amounts of coal. By modifying the reactor chamber in this way these reactors can be used to treat 1.5 to 30 grams of coal at a time.

After loading, the reactor is placed horizontally so that there is a space above the coal for the flow of steam and gases evolved during treatment. The reactor is attached to a source of helium and/or steam and a thermocouple is wired to its midpoint. The reactor, including valves at either end, is wrapped in heating tape. A flow of helium at 50 atm is established through the reactor. With helium flowing at a minimal rate, controlled by an outlet needle valve, the reactor is heated to 300°C. This is above the condensation point of the superheated steam (265°C). Helium is then replaced by steam at 50 atm and the flow of steam is adjusted so

¹ We thank R. Liotta of Exxon Research and Engineering Corp. for providing this coal sample.

² Elemental analyses were performed by Galbraith Laboratories, Knoxville, Tennessee.

that there is a steady discharge of steam from the exit tube. The reactor is further heated to the desired treatment temperature in the first 2 to 3 minutes of steam flow. Treatment temperatures are in the range of 300 to 360°C. The temperature is maintained for the desired length of time (typically 15 minutes) by adjusting the voltage to the heating tape. To stop treatment, the heating tape is turned off and the steam flow replaced by helium. The reactor is allowed to cool to room temperature. The flow of helium is maintained until there is no detectable moisture in the reactor effluent. This is determined by placing a cold metal object in the flow of helium and observing any condensation which forms or by placing a piece of indicating Dryerite in the helium flow. Both inlet and outlet valves are then shut, and the tube is removed from the source of the gas.

Swelling

Swelling experiments were carried out as described in Green, et al. (1984). Samples of approximately 1g of coal were measured into 10mm X 80mm centrifuge tubes and covered with neoprene stoppers. The samples were centrifuged at 1700 rpm for approximately 10 minutes to settle the dry coal. The height of the sample (h_1) was then measured by use of an external rule. Solvents were added to the tube and the tubes were capped and shaken until there was complete homogeneity. The tubes were left to stand 18 hours and then were centrifuged again until a constant height of the solid material was attained. In the case of pyridine, because of the dark color of the solution, the tube was turned upside down in order to read the height of the solids. Experiments were done under N_2 in a glove bag unless the sample was to be deliberately exposed to air, then no precautions were taken in handling the sample in any step of the above procedure.

DRIS

Diffuse reflectance infrared spectroscopy (DRIS) was used to analyze both raw and treated coal samples which had been ground to pass 200 mesh before treating. Samples after treatment were ground and resieved, under a N_2 atmosphere, to pass 200 mesh. DRIS spectra were obtained using a Nicolet 7199 instrument. Samples were handled under nitrogen in a glove bag directly attached to the sample chamber of the machine and a purge of N_2 was maintained through the instrument. Data were acquired over approximately 13 minutes. The number of data points was 8192 over 1000 scans.³

O-Methylation

O-methylation of the treated coal was performed following procedures described by Liotta, et al. (1981). Typically, one gram of coal was weighed into a 250 ml round bottom flask immersed in an ice bath; 2.9 mmoles of tetra-n-propylammoniumhydroxide (TnPAH) were added. This was in slight excess of the 2.5 mmoles of acidic sites that were found, by titration, to be in raw coal. For treated coal the amount of TnPAH added was approximately 2.5 times this amount. Freshly distilled tetrahydrofuran (50-60 ml) was added while the contents were stirred with a teflon covered magnetic stirring bar.

³ We thank Mr. E.W. Sheppard of Mobil Research and Development for his assistance in obtaining and interpreting the DRIS spectra.

Labeled methyl iodide ($\text{C}^{13}\text{H}_3\text{I}$), in 20% excess of the amount of TnPAH that was used, was added. Stirring was continued for 72 hours. The workup entailed removing the THF on a rotovaporizer and washing the product with 250 ml of a hot methanol and water solution (1:1 by volume). The contents of the flask were then vacuum filtered on a 80 micron filter and washed with four liters of hot water. The coal was dried in a stream of nitrogen, transferred to a soxhlet extractor, and washed with distilled water for five days. The coal was then dried in a stream of nitrogen and in a vacuum oven at 90°C for 4 hours. Stable carbon isotope analyses were performed on these samples by Coastal Science Laboratories of Austin Texas using combustion techniques.

EXPERIMENTAL RESULTS

Swelling

Values of swelling ratios for raw and treated coals are given in Table 1. The measured increase in volume depends on the amount of material present in the solid phase. If during solvent swelling some of the solid is lost by extraction, the final volume is that of a reduced amount of material. An approximate correction for this loss can be made by dividing the swelling ratio by the fraction of starting material unextracted. This correction has been made to the values in Table 1 using average values obtained in room temperature extraction of the same samples (Graff and Brandes, 1987). By accounting for the amount of material in the solvent the swelling values of the solid phase are made comparable from one sample to the other.

In pyridine and in water the steam treated coal swells more than the raw coal or the helium treated coal by a considerable amount. In benzene the raw coal swells little more than helium or steam treated coals. Pyridine breaks hydrogen bonds, benzene does not. The difference between the degree of swelling in pyridine and in benzene is a measure of the amount of hydrogen bond cross-linking. The smaller the difference the fewer the number of hydrogen bond cross-links. In Table 2 the difference values are listed. The amount of hydrogen bond association is high for steam treated coal protected under nitrogen. The helium treated sample shows less hydrogen bonding than raw coal.

Extraction in pyridine destroys essentially all of the coal's hydrogen-bond cross-links so that subsequent swelling experiments reveal the backbone structure of the coal. It is apparent from these data that there is an increase of the degree of hydrogen bonding in the treated coal as compared to the raw and helium treated samples even in the backbone of the coal after room temperature extraction. Helium treated coal, again, shows the least amount of hydrogen bond association.

When steam treated coal is exposed to air and then swelled in pyridine the swelling ratio is decreased to below that for raw coal. Exposure of helium treated coal to air has no effect on the swelling ratio. The decrease in swelling indicates an increase of cross-links of any kind. For the air exposed samples the formation of oxygen cross-links is a possibility.

To wet steam treated coal with distilled water, 0.05% by weight xanthum gum, a polymeric thickening agent was added. When swelling experiments were conducted in water, the increase of swelling for the

treated sample over the raw coal was startling (Table 1). There is a twofold increase in the swelling value of the steam treated coal over the raw coal.

DRIS

Samples of coal treated in steam and helium, raw coal, and raw coal dried under vacuum at 90°C were examined by DRIS. There are no apparent differences among the samples in any region of the spectra except in the region attributed to -OH species (3200-3700cm⁻¹) (Fig. 1). All of the spectra generated display two bands in the hydroxyl region (Fig 2). In the raw coal sample the broad peak at 3300cm⁻¹ predominates and mostly occludes the one at 3550cm⁻¹. Vacuum drying of the coal sample at 90°C does not alter this ratio. In all the treated coal samples the peak height ratio of the two is reversed. The peak at 3550cm⁻¹ is clearly visible. The effect is evident whether the coal is treated in helium or steam, and it is not effected by exposure of the samples to air for brief times (less than ten minutes).

O-Methylation

The values for the relative enrichment in C-13 are given in Table 5 for raw Illinois No.6 coal, raw coal O-alkylated with labeled methyl iodide, helium treated coal, O-alkylated, and steam treated coal, O-alkylated. It is readily apparent that the steam treated coal after alkylation with the labeled methyl iodide is almost doubly enriched in C-13.

DISCUSSION

Swelling

Swelling data show that it is not a reduction of hydrogen bonding in steam treated coal that is responsible for the steam treated coal's behavior. On the contrary there is an increase in hydrogen bonding in steam treated coal. Because of the ability of water and water miscible solvents to swell the coal and the inability of water insoluble solvent to swell the coal the following conclusions have been drawn. The steam treated coal is not of the same structural makeup as the raw coal, nor as the helium treated coal. One may postulate two different structures for the modified coal. One interpretation of the data which can be made does not include any chemical interaction of the water and the coal. Residual water not removed in the drying step of the treatment process acts to hold open the coal structure. The water is miscible in pyridine and water and thus the coal swells. A possible alternative structure consists of newly formed phenolic groups created in the high pressure steam treatment. The phenols may form hydrogen bonds to each other and to the coal structure. These sites readily accept the water or water miscible solvent and cause the coal to swell more than the native structure.

DRIS

The apparent shift in the ratio of the two peaks which appear between 3200 and 3700cm⁻¹ in the IR spectrum provides a significant clue in determining what changes have occurred in the structure of the coal.

The broader of the two peaks, centered around 3300cm⁻¹, is

usually associated with phenolic, alcoholic, acidic, mineral and aqueous entities in the coal structure (Fuller and Smyrl, 1985). There is no reason to believe that there is a change in the mineral matter of the coal due to steam treatment. Therefore, to interpret the observed differences between raw coal spectra and steam treated coal spectra in this region we must focus our attention on alcoholic entities, specifically phenolic -OH. The sharper peak at 3550cm^{-1} in our samples may be attributed to intramolecularly bound -OH, which are higher energy, more tightly bound species. These materials have only a small amount of hydrogen bonding to other species. A comparison of these two peaks in the spectra of raw coal and treated coal shows that there is a shift in the ratio of these two peaks. It appears that the higher energy peak increases over the lower energy one. There are three ways to interpret these observations:

1. If the total number of hydroxyl groups remains fixed, then high energy species have increased at the expense of low energy species. This implies a weakening of secondary bonding, principally hydrogen bonding.

2. A decrease in the total number of hydroxyl groups would also imply a decrease in hydrogen bonding.

3. If the shift is interpreted as principally resulting from an increase in the number of high energy hydroxyl groups (the total number of hydroxyl species increasing) the amount of hydrogen bonding in the coal could have increased. The new primary hydroxyl groups (e.g. phenols), if formed at sites which in the original coal were covalently bound, would hold the structure apart and prevent reformation of the covalently cross-linked structure. This leaves a partially depolymerized coal bound only by hydrogen bonds at the new hydroxyl functionalities.

All three of these interpretations are consistent with the tenet that the coal is partially depolymerized in steam treatment. Combined, however, with the evidence from the swelling data, which indicates an increase in the degree of hydrogen bonding in the coal, the third of the above interpretations is considered most likely.

O-Methylation

The increased hydrogen bonding exhibited in the treated coal by the swelling experiments and the presence of a shift in the hydroxyl region of the infrared spectrum strongly indicate the presence of more OH functionality. The O-alkylation procedure, first described by Liotta (1979) has proven to be an excellent quantitative way to measure the relative abundance of these groups. The use of a traceable alkylating agent, in our case C-13 labeled methyl iodide, allows for an accurate count of the number of reacted groups. Although NH, SH, and COOH sites will also react with the alkylating agent it is safe to assume that these groups are present only in minor amounts in the coal to start with and are not altered or removed in steam treatment.

The incorporation of almost twice as many labeled C-13 groups in the steam treated coal as the raw coal and the helium treated coal substantiates the speculation that steam treated coal contains more OH groups.

CONCLUSIONS

From these findings it is clear that steam treated coal has a structure altered from the raw starting coal. There is an inclusion of OH functionality in the structure which accounts for the increased hydrogen bonding and the shift in the IR spectrum. A tentative hypothesis for the increase in the extraction yields as well as the pyrolysis yields (both previously reported) is that these new hydroxyl sites are formed during the steam treatment at places in the original coal which were covalently bound. This leaves a partially depolymerized coal, cross-linked only by relatively weaker hydrogen bonds. These bonds are highly susceptible to water and water miscible solvents.

The quality of the resulting fuel produced from processing of this steam treated coal is expected to be substantially improved over that which would be obtainable from a raw coal. The weakened bonding structure of the coal will promote the production of lower molecular weight fragments. These, in turn, will be easier to upgrade. Preliminary findings from an investigation now underway suggest that although there is an increase in the number of hydroxyl sites it is at the expense of other organic oxygen in the coal. In other words the total organic oxygen content of the coal does not increase on steam treatment. This may indicate that the coal not only will be more easily upgraded as is mentioned above, but also, that this treated coal is not a worse feed for further processing than raw coal as it does not contain additional oxygen. A final point to be made is that the improved properties of steam treated coal are achieved with no expenditure of elemental hydrogen. This gives steam treated coal an economic headstart in upgrading to a more useful fuel.

ACKNOWLEDGEMENTS

The use of the o-methylation technique was suggested by Martin Gorbaty of Exxon Research and Engineering Corp. We are grateful to him and to Michael Siskin, also of Exxon Research & Engineering, for helpful discussions in the course of this work.

This work was sponsored in part by the USDOE under contract No. DE-AC21-84MC21315; W.-S. Liou, Project Manager; and M. Gbate, Chief of the Gasification and Combustion Branch.

REFERENCES

- Fuller, E.L. Jr. and N.R. Smyrl (1985), "Chemistry and Structure of Coal: Diffuse Reflectance IR Spectroscopy Equipment and Techniques", Fuel, **64**, 1143.
- Graff, R.A. and S.D. Brandes (1984), "Coal Liquefaction by Steam Pyrolysis", ACS, Division of Fuel Chemistry Preprints, **29**, (2), 104.
- Graff, R.A. and S.D. Brandes (1987), "Modification of Coal by Subcritical Steam: Pyrolysis and Extraction Yields", Energy and Fuels, **1**, 84.
- Green, T.K., J. Kovac, and J. Larsen (1984), "A Rapid and Convenient Method for Measuring the Swelling of Coals by Solvents", Fuel, **63**, 935.
- Liotta, R., K. Rose, and E. Hippo (1981), "O-Alkylation Chemistry of Coal and Its Implications for the Chemicals and Physical Structure of Coal", J. Org. Chem, **46**, 277.
- Liotta, R. (1979), "Selective Alkylation of Acidic Hydroxyl Groups in Coal", Fuel, **58**, 725.

Table 1

Swelling Ratios (O) for Raw and Treated*
Illinois No. 6 Coal

<u>Solvent</u>	<u>Raw</u>		<u>Steam Treated</u>		<u>Helium Treated</u>		
	<u>In Air</u>	<u>Extracted</u>	<u>Under N₂</u>	<u>In Air</u>	<u>Under N₂</u>	<u>In Air</u>	<u>Extracted</u>
Pyridine ⁺	2.80	1.95	3.01	2.46	1.88	2.24	1.68
Benzene	1.13	1.35	1.06	1.00	1.12	1.00	1.24
Water	0.98	1.21	1.83	1.84	0.98	1.56	1.23

*Treatments in steam and helium for 15 minutes at 50 atmospheres

+Corrected for extraction losses

Table 2
Difference in Swelling Ratio (Q)
of Pyridine and Benzene Swollen Samples

	$Q_{\text{pyr}} - Q_{\text{benz}}$
Raw	
In Air	1.67
Extracted	0.60
Steam Treated	
Under N ₂	1.95
In Air	1.46
Extracted	0.76
Helium Treated	
Under N ₂	1.24
In Air	1.18
Extracted	0.44

Table 3
Relative Ratio of C-13/C-12
In O-Alkylated Coals

<u>Sample</u>	<u>Ratio</u>
Raw Illinois No.6	-25*
O-methylated Raw Coal	4900
O-methylated Steam Treated Coal	8240*
O-methylated Helium Treated Coal	3789

*Average of two values

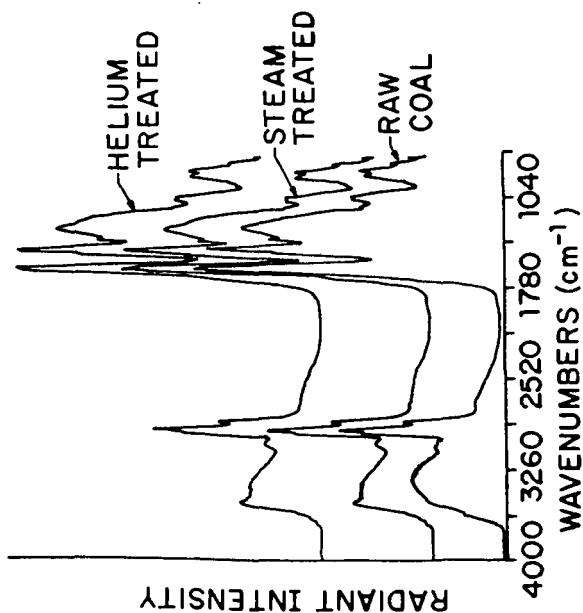


Figure 1. Comparison of DRIS Spectra of Treated Illinois No. 6 Coal

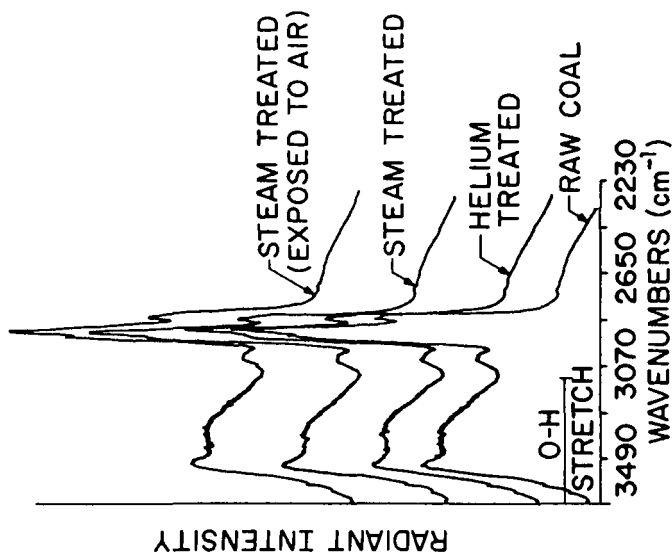


Figure 2. Comparison of the OH Stretching Region of Various Treated Illinois No. 6 Coal